

Name of Project: The Use of Microgravity To Emulate
Three-Dimensional Tissue Interactions In Colorectal Cancer
Metastasis

NAG 9-650

1N-52-CR

Grant #: NAG 9-650

Principal Investigator: J. Milburn Jessup, M.D.

University Affiliation: Laboratory of Cancer Biology,
Department of Surgery,
Beth Israel Deaconess Medical
Center, West Campus, 21-27
Burlington Ave., Boston, MA
02115 and Harvard Medical
School, Boston, MA 02215.

Period: 3-1-93 to 2-28-97, inclusive

Title: The Use of Microgravity To Emulate Three-Dimensional Tissue Interactions In Colorectal Cancer Metastasis

Project Objectives: The hypothesis of this ground-based project was that simulated microgravity may be used to recreate with high fidelity the in vivo environment in tissue culture. The objectives were to determine whether 1) simulated microgravity induces differentiation within poorly differentiated human colon carcinoma cells that are similar to that observed in experimental metastases in vivo in nude mice and 2) the use of simulated microgravity helps define the experimental metastatic potential of human colorectal carcinoma.

Patents or Inventions: None

Work Accomplished:

Objective 1: Differentiation Induction in MIP-101 Human Colon Carcinoma Cells

A. CEA Expression is Associated With Differentiation

The original focus of this application was on mechanisms of differentiation. We have been interested in the role of carcinoembryonic antigen (CEA) in colorectal carcinoma. CEA is a 180 kDa glycoprotein that is a member of the immunoglobulin super gene family. It also has its own subfamily with such homologous members as nonspecific cross-reacting antigen (NCA) and biliary glycoprotein (BGP). NCA exists in two isoforms of 50 and 90 kDa that share the same protein but have different degrees of glycosylation. BGP has four isoforms which are created by alternate splicing of mRNA. The importance of this is that all three proteins act as cell adhesion molecules in vitro. Since MIP-101 cells did not display CEA either at the protein or mRNA level, we studied whether growth in the rotating wall vessel (RWV) would lead to an increase in CEA expression. This is important because work by other investigators has shown that CEA expression is enhanced in cells as they are induced to differentiate by such inducers as sodium butyrate.

One of the first parts of this project was to set up appropriate controls for the RWV cultures. MIP-101 cells grow well in monolayer culture, remaining in log phase until the medium is exhausted through cell overcrowding (Appendix I). We then determined whether MIP-101 cells grow in static 3-D growth by culture on a non-stick surface. Tissue culture flasks or Petri dishes were coated with poly-HEMA a non-stick agent that forces cells to round up and grow in spheroids. In this condition, MIP-101 cells form three-dimensional aggregates that have loose intercellular connections. However, the only difference between these static 3-D cultures and the RWV cultures is the rotation used for suspension. Thus, static 3-D cultures refer to MIP-101 cells grown as loose aggregates on a sterile non-stick surface. The proliferation of MIP-101 cells either in static 3-D or in the RWV was less than that of the monolayer cultures for the first 200 hours.

When MIP-101 cells were cultured in the RWV for 3-6 days, we found that there was an increase by immunoperoxidase staining of cells in RWV cultures but not in monolayer or in static 3-D cultures. These last cultures are the appropriate controls because cells are allowed to grow in three dimensions but on a non-stick surface so that they pile up and form 3-D structures. Results were even more striking when the cultures were continued for longer periods of time. The MIP-101 cells displayed considerable amounts of immunoreactive CEA at 8-14 days of culture in the RWV. These results are in press in "In Vitro Cell Growth and Differentiation" and a preprint is enclosed (Appendix I). This lead us to conclude that differentiation was induced in the RWV and that this resulted in enhanced expression of CEA, presumably at both the gene transcript and the gene product level.

This conclusion was not entirely correct. Western blots were performed that demonstrated that there was an increase in the 180 kDa form of immunoreactive CEA proteins. However, there

was an even greater increase in the amount of NCA 50-55 kDa produced in the MIP-101 RWV cultures. Immunoperoxidase studies had been performed on tissue sections with an antibody that was considered to be specific for the 180 kDa CEA and not to react with NCA. However, we developed a competitive PCR technique that allowed us to measure the absolute levels of gene transcripts and found that the levels of CEA gene transcripts were barely detectable limits in monolayer cultured cells and did not increase in cells cultured in the RWV for 6 days. CEA mRNA levels did not increase in either monolayer or static 3-D cultures. However, NCA gene transcripts were detected in MIP-101 monolayer cultures and increased 40-fold in 6 day RWV cultures. There was a smaller increase in monolayer and static 3D cultures. Thus, we have the interesting conundrum that gene transcripts for NCA are increased in the RWV to a much greater extent than CEA but that the amount of CEA is also increased presumably through enhanced translation of barely detectable levels of gene transcripts.

Since the amount of CEA gene transcript was extremely low, we have not pursued this further, however, this is an interesting problem that should be further explored because it suggests that there is differential gene regulation in a set of genes that was thought to be regulated coordinately.

B. Cell Proliferation

During the studies of CEA expression it was noticed that MIP-101 cells in the RWV cultures were continually enlarging. This occurred as the culture proliferation rate gradually decreased (Figure 1 Below). When flow cytometry was performed, the MIP-101 cells in the RWV were actually arresting in the G2 phase of the cell cycle. For cells to proliferate they have to progress from a resting state (G0) into G1, then into S phase where DNA is synthesized, a second gap phase (G2) and then into mitosis to begin the cycle all over again. DNA damage from radiation, genotoxic agents and chemotherapeutic agents often cause cell cycle arrest in G1 or G2. However, we did not expect to find cells accumulating in G2. We have subsequently analyzed this and have found that in MIP-101 cells this G2 arrest is associated with extremely high levels of cyclin B, low p34^{cdc2} kinase activity and low CDC 25C protein levels. We have subsequently performed more RWV cultures with other human colon carcinoma cell lines and believe that this G2 arrest is a common event. This has lead to the development of a subsequent NRA grant application that was successfully competed that focuses on the effect of the RWV on the cell cycle. The G2 arrest does not occur in monolayer culture or in static 3-D cultures (Figure 2 Below). These alterations that lead to a G2 arrest are not present in cells proliferating in monolayer culture or in static 3D culture. Therefore, it appears that this may be a response of the MIP-101 cells to rotation. This may be extremely important because many carcinoma cells die as they traverse the circulation. The growth and suspension within the circulation may be quite similar to the RWV. Thus, this may allow us to investigate events that occur more commonly than we might have otherwise suspected. A manuscript is in preparation.

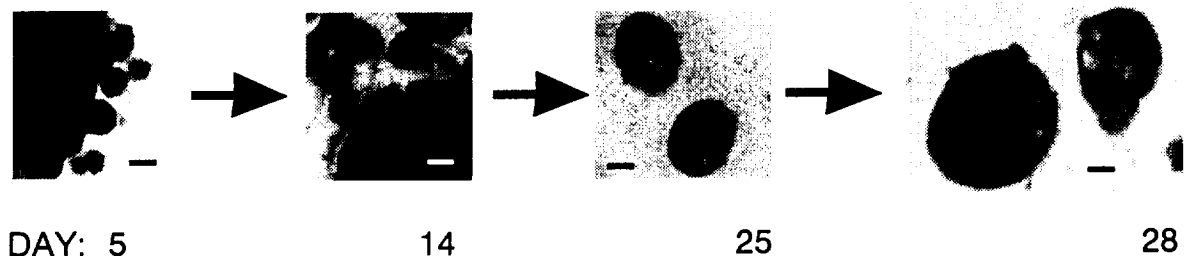
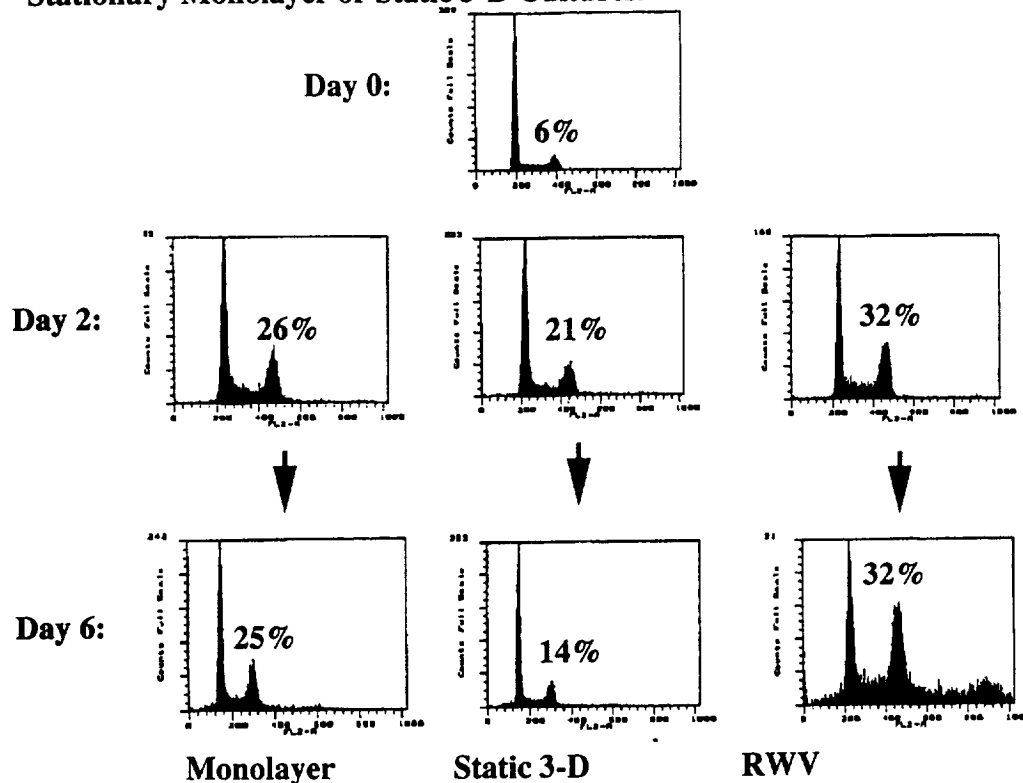


Figure 1. MIP-101 Cells Progressively Enlarge In The RWV Cultures.

Cultures. All Cells Observed in RWV cultures on the Day Indicated With the Same 40x Objective On Nikon Diaphot Fitted With An Optronics CCD Integrating Video Camera and Without Any Other Image Size Manipulation. Cells cultured as in Figure 1, fixed and stained from samples harvested on date indicated. H & E stain. Cells detach from beads, grow in suspension, and progressively enlarge. — is 10 μ .

Figure 2. MIP-101 Cells Accumulate in G2/M in Rotating RWV Cultures But Not in Stationary Monolayer or Static 3-D Cultures.



Legend: MIP-101 cells were cultured as described in Figure 1 in T-25 flasks (Monolayer), on non-stick Petri dishes to form stationary spheroids (Static 3-D), and in the RWV. Samples were harvested as described for Figure 3 on the day indicated and analyzed by flow cytometry. The DNA histograms indicate that Static 3-D cultures are similar in distribution to the original inoculum (Day 0). Monolayer cultures display some increase in the G2 fraction but the RWV culture displays not only increased G2/M but also an 8 C population.

C. Upregulation Of Expression of CD44

The formation of 3-D aggregates has lead to fundamental understanding of chemotherapy resistance. Dr. Robert Kerbel and his associates in Toronto have found that growth in static 3-D cultures by some tumor cells is associated with resistance to chemotherapy. The morphology of spheroids is essential for this resistance because only spheroids that form compact and dense structures are resistant to chemotherapy. Dr. Kerbel has found that hyaluronidase inhibits compaction of spheroids and increases the sensitivity of these tumor cells to chemotherapy. Since hyaluronic acid is the ligand for CD44, we have examined the relationship between CD44 expression and the formation of spheroids in the RWV and static 3-D cultures. We have found that in the RWV culture and to a lesser extent in static 3-D culture the expression of CD44 and its variants is markedly enhanced in MIP-101 cells. This is important because we would expect that MIP-101 cells would form relatively loose spheroids because they have low levels of CD44 expression. The spheroids formed in the RWV tend to be loose. We have created transfectants that overexpress CD44 and are beginning to assess the effects of this overexpression on growth regulation. These studies may demonstrate that CD44 does, in fact, have a role in the growth of

cells in tumors especially as they form metastases and 3 dimensional growth at distant sites. We are very interested in the how this occurs and the RWV may provide us unique insights into successful tumor cell growth.

Objective 2: To Use Simulated Microgravity To Define The Experimental Metastatic Potential Of Human Colorectal Carcinoma.

A difficult aspect of the analysis of the process of metastasis is to determine how cells interact with the host parenchyma. In the past, investigators have cultured tumor cells with fragments of normal tissue and then assessed whether tumor cells that adhered to or grew in these fragments displayed any increase in metastatic potential when put back into an experimental host. Experiments involved placing tumor cells that were selected for either adherence or growth on these fragments back into an animal host to determine whether the metastatic potential of the cells was increased by the selection of an interaction with a host. This approach generally demonstrated that either adherence or some other property of growth within the fragments for the metastatic site selected for precursor cells more metastatic than the parental unselected population. Unfortunately, the degree of molecular analysis allowed by this type of an approach was somewhat limited and gave way to approaches that allowed more defined molecular properties. However, when combined with RWV cultures, this approach may allow for a more dynamic interaction and a better understanding of how tumor cells interact with the host parenchyma.

We began our studies by determining whether normal mouse liver fragments could survive in the RWV. Liver has been a difficult organ to grow and attempts to use either defined factors, selected subpopulations of normal liver cells or other approaches have generally not been satisfactory. However, when we cultured dissected 2-3 mm pieces of mouse liver in the RWV, we found that these fragments were viable as determined by calcein AM staining as well as by routine histopathologic examination (Appendix 2). These liver fragments remained viable for as long as 14 days in the RWV. This now permitted us the opportunity to determine whether or not tumor cells that have different metastatic potential for growth in mouse liver might interact differently with this viable liver culture system.

We have determined with radioisotope tracer studies and intravital fluorescence videomicroscopy (IVFM) that human colorectal carcinoma cells colonize mouse liver with different degrees of success. Highly metastatic cells are those in which tumor cells grow in 50% of mice after 2×10^6 viable tumor cells are injected into the spleen and enter the liver through the portal vein. Weakly metastatic cells are those that form liver colonies in less than 20% of mice after a similar number of viable tumor cells have been injected into the spleen. We found that metastatic potential is proportional to the number of tumor cells that remain viable at 24 hr after implantation. Thus, nearly ten-fold more highly metastatic CX-1 cells survive in the liver 24 hr after tumor implantation than weakly metastatic Clone A cells (Appendix 2). Thus, a postulate was that survival of metastatic precursor cells was simply a result of being able to grow and proliferate within normal hepatic parenchyma. However, both CX-1 and Clone A cells proliferated at the same rate when co-cultured with normal mouse liver fragments cultured in the RWV (Appendix 2). This suggests that normal mouse liver is not more toxic to weakly metastatic cells than highly metastatic cells. It also suggests that the events that distinguish highly from weakly metastatic carcinomas are due to interactions with a hepatic parenchyma that is altered during the implantation of the cancer cells. As a result, experiments were started to examine how the act of implantation altered the physiology of mouse liver so that it was more toxic to weakly metastatic tumor cells than to highly metastatic tumor cells.

Before performing the RWV cultures with ischemic liver fragments, however, we attempted to determine whether endothelial cells were toxic for Clone A cells. The IVFM studies

suggested that when human colorectal carcinoma implant in the liver they primarily contact the endothelial cells lining the hepatic sinusoid. Earlier studies by our group had shown that Kupffer cells, the fixed macrophages of the liver, were not toxic to any of the human colorectal carcinoma cell lines unless they were activated by cytokines. In addition, the pit cells which are the intrahepatic natural killer cell population did not lyse human colorectal carcinoma cells unless activated by cytokines. When hepatic sinusoidal endothelial cells were isolated and established as primary cultures, they were cytotoxic to the weakly metastatic Clone A cells but not the CX-1 cells (Appendix 3).

The IVFM studies suggested that the hepatic sinusoid became ischemic after tumor cell implantation just as an embolus causes ischemia with the microcirculation. This ischemia causes a transient loss of hepatocytes and endothelial cells which then produces a change in the hepatic microenvironment that favors the growth of CX-1 and is deleterious to Clone A. The RWV was used to model this by taking fragments of mouse liver made ischemic for 3 min prior to harvest by clamping the blood supply in the porta hepatis before harvesting the mouse liver. The mouse liver fragments were cultured for 24 hr in the RWV and the hepatocytes remained viable because they metabolized calcein AM. However, the endothelial cells that lined the sinusoids were lysed and the Kupffer and other nonparenchymal cells also disappeared. When Clone A and CX-1 cells were now cultured with these ischemic liver fragments, the Clone A cells were killed while the CX-1 cells remained viable. This was important because it now suggests that the ischemic alterations which occur in the hepatic microcirculation after tumor cells implant in the sinusoid lead to changes in the host microenvironment that are more toxic to weakly metastatic Clone A cells than to highly metastatic cells. This is an extremely important observation because it suggests that metastasis may depend upon the response of the tumor cell to ischemia within the microcirculation. We have gone on to demonstrate that inhibitors of nitric oxide synthesis do not alter the morphologic changes within these ischemic liver fragments but, in fact, prevent these ischemic liver fragments from being toxic to Clone A cells. Thus, the toxicity of ischemia may involve a nitric oxide-dependent event that leads to tumor cell death. As a result of this NASA -sponsored work in the RWV, we have now formulated a new hypothesis concerning the role of reactive oxygen species in metastasis. A manuscript is in preparation on the effects of ischemia on normal mouse liver cultured in the RWV and its effect on tumor cells.

PUBLICATIONS:

1. Shoji Y, Mizoi T, Edmiston K, Nachman A, Ford R, and Jessup JM. Hepatic sinusoidal endothelial cells inhibit colorectal carcinoma cell proliferation through a nitric oxide mechanism. *Surg. Forum* 1996;47:526-529.
2. Ishii S, Mizoi T, Kawano K, Cay O, Thomas P, Nachman A, Ford R, Shoji, Kruskal JB, Steele G Jr, Jessup JM. Implantation of human colorectal carcinoma cells in the liver studied by in vivo fluorescence videomicroscopy. *Clin & Exp Mets* 1996;14:153-164.
3. JM Jessup, Y Shoji, T Mizoi, KH Edmiston. Hepatic sinusoidal endothelial cells (SEC) eliminate metastatic cells by a nitric oxide-dependent mechanism. *Molec. Biol Cell* 1996;Suppl 7:664a. Abstract #3864, Presented at the ASCB meeting, San Francisco, CA, Dec, 1996.
4. KH Edmiston, EB Leof, A Nachman, JM Jessup. G2 arrest induced by rotational shear stress. *Molec. Biol Cell* 1996;Suppl 7:356a. Abstract #2076, Presented at the ASCB meeting, San Francisco, CA, Dec, 1996.

5. JM Jessup, KH Edmiston, EB Leof. Rotation Induces G2/M Checkpoint Restriction In Anchorage-Independent Cells Lacking p21WAF1. Presented at the Keystone Conference on Control of the Cell Cycle, Keystone, Co, Jan, 1997.
6. JM Jessup, KH Edmiston, EB Leof, M. Su. Simulated Microgravity induces G2 arrest in Colon Carcinoma Cells. Presented at the Investigators Working Group Meeting at Houston, TX Feb, 1997.
7. JM Jessup, KH Edmiston, A. Nachman. R. Ford. The Use of the NASA Bioreactor to Cultivate Liver to Assess Microenvironmental Effects on Colorectal Metastasis. Presented at the Investigators Working Group Meeting at Houston, TX Feb, 1997.
8. Jessup JM, Brown D, Fitzgerald W, Ford RD, Nachman A, Goodwin TJ, Spaulding G. Induction of Carcinoembryonic Antigen Expression in a Three-Dimensional Culture System. *In Vitro Cellular & Developmental Biology*. 1996 (In Press).
9. Edmiston K, Shoji Y, Mizoi T, Ford R, Nachman A, Jessup JM. Role of Nitric Oxide and Superoxide Anion in Hepatic Endothelial Cell Toxicity to Human Colorectal Carcinomas. *Cancer Research* (Submitted) 1997.

Appendices

1. Jessup JM, Brown D, Fitzgerald W, Ford RD, Nachman A, Goodwin TJ, Spaulding G. Induction of Carcinoembryonic Antigen Expression in a Three-Dimensional Culture System. *In Vitro Cellular & Developmental Biology*. 1996 (Preprint).
2. Ishii S, Mizoi T, Kawano K, Cay O, Thomas P, Nachman A, Ford R, Shoji, Kruskal JB, Steele G Jr, Jessup JM. Implantation of human colorectal carcinoma cells in the liver studied by in vivo fluorescence videomicroscopy. *Clin & Exp Mets* 1996;14:153-164.
3. Edmiston KH, Shoji Y, Mizoi T, Ford R, Nachman A, Jessup JM. Role of nitric oxide and superoxide anion in hepatic endothelial cell toxicity to human colorectal carcinomas. *Cancer Research* (submitted).

Master

INDUCTION OF CARCINOEMBRYONIC ANTIGEN EXPRESSION IN A THREE-DIMENSIONAL CULTURE SYSTEM

J. M. JESSUP,¹ D. BROWN, W. FITZGERALD, R. D. FORD, A. NACHMAN, T. J. GOODWIN, AND G. SPAULDING

BETH ISRAEL DEACONESS MEDICAL CENTER

Laboratory of Cancer Biology, Department of Surgery, Deaconess-Hospital, Boston, Massachusetts 02215 (J. M. J., R. D. F., A. N.); Krug Life Sciences, Houston, Texas 77058 (D. B., W. F.); Biotechnology Program, Johnson Space Center, National Aeronautics and Space Administration, Houston, Texas (T. J. G., G. S.)

(Received 26 August 1996; accepted 27 August 1997)

is this correct? Jessup

SUMMARY

MIP-101 is a poorly differentiated human colon carcinoma cell line established from ascites that produces minimal amounts of carcinoembryonic antigen (CEA), a 180 kDa glycoprotein tumor marker, and nonspecific cross-reacting antigen (NCA), a related protein that has 50 and 90 kDa isoforms, in monolayer culture. However, MIP-101 produces CEA when implanted into the peritoneum of nude mice but not when implanted into subcutaneous tissue. We tested whether three-dimensional (3D) growth was a sufficient stimulus to produce CEA and NCA 50/90 in MIP-101 cells, because cells grow in 3D *in vivo* rather than in two-dimensions (2D) as occurs in monolayer cultures. To do this, MIP-101 cells were cultured on microcarrier beads in 3D cultures, either in static cultures as nonadherent aggregates or under dynamic conditions in a NASA-designed low shear stress bioreactor. MIP-101 cells proliferated well under all three conditions and increased CEA and NCA production three- to four-fold when grown in 3D cultures compared to MIP-101 cells growing logarithmically in monolayers. These results suggest that 3D growth *in vitro* simulates tumor function *in vivo* and that 3D growth by itself may enhance production of molecules that are associated with the metastatic process.

Key words: Author: Please supply up to 6 key words.

INTRODUCTION

Carcinoembryonic antigen (CEA) is a 180 kDa glycoprotein that is released by human colonic epithelial cells into either the lumen of the gastrointestinal tract or the circulation. The function of CEA is not well-defined but as a member of the immunoglobulin supergene family it may be involved with intercellular adhesion (19). Interestingly, an elevated concentration of CEA in the blood of patients who undergo resection of an apparently localized bowel carcinoma is often associated with the presence or subsequent appearance of metastases in the liver or lung (7,27). Experimental hepatic metastasis by human colorectal carcinomas in athymic nude mice is also associated with the serum level of CEA in the patient from whom the tumor is obtained (4,11) or CEA expression by the tumor cells (25). While CEA may be an adhesion molecule, it also has a humoral effect on metastasis because systemic pretreatment with CEA increases the ability of human colorectal carcinoma cells to colonize the liver, even when the neoplasm does not itself produce CEA (14). Thus, CEA is associated with the metastasis of colorectal carcinoma cells and conditions that increase the production of CEA by colorectal cancer cells may increase their potential for metastasis.

Poorly differentiated MIP-101 human colorectal carcinoma cells secrete little CEA *in vitro* in monolayer culture (26). Monolayer cultured MIP-101 cells form tumor nodules when implanted in subcutaneous tissue but do not produce either CEA or spontaneous me-

tastases (26). Furthermore, monolayer cultured MIP-101 cells rarely produce experimental metastases in liver or lung when injected intrasplenically or intravenously into nude mice (26). However, MIP-101 cells implanted in the peritoneum of nude mice develop nodules that produce CEA and form spontaneous hematogenous metastases in liver and lung (26). Because MIP-101 cells were originally isolated from the peritoneal cavity of a patient (17), they appear to produce CEA and spontaneous metastases when implanted in the same or orthotopic site from which they were harvested. The conventional interpretation of these findings invokes the seed-soil hypothesis of Paget (21), which states that the metastatic precursor cell (the right seed) will only produce a metastasis if planted in the appropriate organ site (the right soil). Thus, the microenvironment of the host permits or even supports the malignant behavior of a cancer. In the MIP-101 model, the microenvironment of the peritoneum appears to actively support the production of CEA and metastases by MIP-101 cells while the microenvironment of the subcutaneous tissue does not.

However, certain characteristics of the malignant phenotype may not depend on the interaction between host and neoplastic cells, but depend instead on the growth of the neoplastic cells in three-dimensional (3D) conformations that mimic the growth pattern of tumor cells *in vivo*. Rak and Kerbel have found that both clonal dominance (22) and resistance to chemotherapy (8) are facilitated when cells grow as 3D spheroids rather than as two-dimensional (2D) monolayers. Furthermore, the behavior of the tumor cells mimics their function *in vivo* without interaction with stromal cells (8).

¹To whom correspondence should be addressed at 110 Francis Street, Suite 3-A, Boston, Massachusetts 02215.

Our purpose was to determine if 3D growth *in vitro* induced the expression of CEA in poorly differentiated MIP-101 human colorectal carcinoma cells that do not produce CEA in monolayer cultures. We tested this hypothesis by evaluating the effect of growth in both static and dynamic 3D culture systems on MIP-101 cells. MIP-101 cells were cultured on microcarrier beads and allowed to form clusters that were then analyzed for the expression of CEA. Previously, we have shown that human colon carcinoma cell lines cocultivated with stromal cells in a NASA-designed 3D culture system induces differentiation and mucin production that is morphologically similar to that in tumors implanted in nude mice (5). Such differentiation and mucin production does not occur in similar cocultures in 2D monolayers (5). Thus, we determined whether 3D growth was associated with the induction of CEA expression in MIP-101 cells that normally only express CEA when implanted orthotopically in nude mice. We compared growth in standard monolayer cultures to that in nonadherent bacterial petri dishes (static 3D culture system) or in the NASA-designed rotating wall vessel (RWV, a dynamic 3D culture system in which cells on microcarrier beads are rotated around the horizontal axis under low shear stress). We observed that production of both CEA and nonspecific cross-reacting antigen (NCA) 50/90 were stimulated by 3D growth.

MATERIALS AND METHODS

Cell cultures. For dynamic 3D cultures, MIP-101 colon carcinoma cells were seeded into four RWVs (Synthecon, Inc., Houston, TX.), with 5 mg/ml Cytodex 3 microcarrier beads (Sigma Chemical Co., St. Louis, MO) at 15 cells per bead and the vessels were adjusted to rotate at 30–35 rpm. As a static 3D culture control, 35-mm nonadherent petri dishes (Optilux, Falcon, Lincoln Park, NJ) were seeded with MIP-101 cells and microcarrier beads at concentrations identical to that in the vessels. In addition, 25-cm² flasks were seeded with MIP-101 cells as a 2D monolayer culture control. All cells were cultured in GTSE-2 medium (6). The experiment was conducted for 14 d and cultures were replenished as needed (every 24 h decreasing to every 8 h). Cell and medium samples were harvested every 4 d. Quick frozen cell samples (1×10^7 cells) were harvested for western blot analysis at Days 0, 8, 12, and 14. Cell samples were harvested on Days 4, 8, and 14 and these specimens fixed in Omnifix (Xenetics, Tuetin, CA) for immunohistochemical studies. At the end of the experiment, growth curves were based on nuclei counts. Frozen cell samples were analyzed on western blots for CEA.

Immunohistochemistry and western blots. Immunohistochemical analysis was performed on paraffin-embedded serial sections of MIP-101 microcarrier bead cultures. Five micron thick sections were prepared by RMC, Inc. (Tucson, AZ) and stained with an anti-CEA monoclonal antibody (Boehringer Mannheim Biochemicals, Indianapolis, IN). The murine primary antibody was identified with a rabbit anti-mouse antibody conjugated with horseradish peroxidase and the reaction developed with diaminobenzidine.

Cells ($\sim 1 \times 10^7$) were extracted in 300 μ l of lysis buffer [60 mM n-Octyl- β -D-glucopyranoside (Sigma), in 25 mM MES, pH 6.5 (Research Organics, Cleveland, OH), in ddH₂O with protease inhibitors] and produced approximately 1 mg/ml of protein. SDS-PAGE was then conducted in 7.5% gels under reducing conditions with 50 μ g of protein loaded per lane. Samples were electrophoresed at 60V for 18 h and transferred to 0.45 μ m nitrocellulose membranes. The western blots were performed with either a murine IgG monoclonal anti-CEA antibody (Zymed Laboratories, San Francisco, CA) or 228.2, a murine IgG raised to NCA 50/90 that was provided courtesy of Dr. J. L. Elting, (Molecular Therapeutics, Miles Laboratories, West Haven, CN). Blots were blocked with 10% dry milk in 0.1% Tween-20 and washed with 0.1% Tween-20 in 0.15 M phosphate-buffered saline (PBS), pH 7.4. The primary antibodies were detected with a sheep anti-mouse IgG conjugated with peroxidase (Amersham Life Science, Buckinghamshire, UK) using the ECL process (Amersham). Quantitation of the relative amounts of CEA or NCA proteins detected in the western blots was achieved by scanning the blots with a flat bed scanner (Microtek 600ZS, Microtek Lab, Torrance, CA) into Photoshop 2.5.1 (Adobe Systems, Mountain View, CA) on a Macintosh Quadra 950 (Apple Computer Co., Cupertino, CA). Images were then ana-

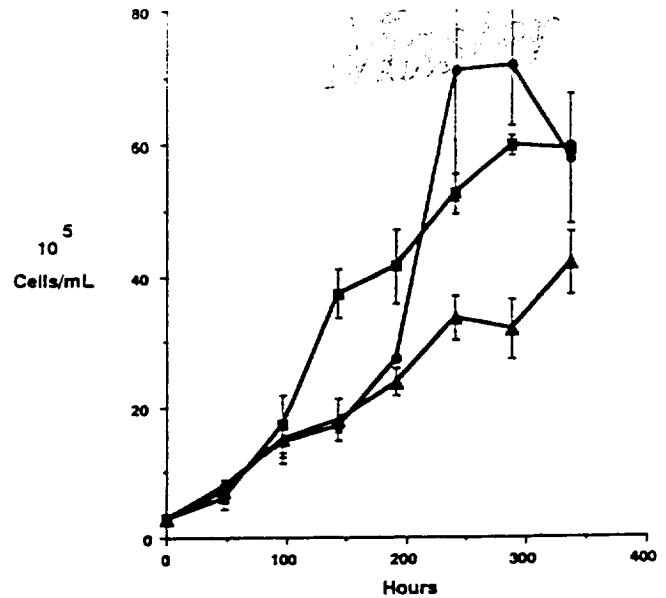


FIG. 1. Growth curves of MIP-101 cells under different conditions. 3×10^5 cells/ml were incubated in monolayers in T-25 flasks (■, T-25) or on Cytodex 3 microcarrier beads in either nonstick petri dishes (●, Petri) or in the NASA-designed rotating wall vessel (RWV) (▲). Results are presented as mean \pm SEM from four separate RWV experiments and two separate experiments each for T-25 and petri dish cultures.

lyzed in IPLab (Signal Analytics Corp., Vienna, VA) and compared to blots of partially purified NCA and CEA proteins as internal standards.

Statistics. Results are presented as the mean \pm SEM. Comparisons among means were performed by one-way analysis of variance using StatView II (Abacus Concepts, Berkeley, CA) on an Apple Macintosh computer (Cupertino, CA). Level of significance was 5% or less.

RESULTS

Growth of MIP-101 cells in vitro. MIP-101 cell cultures were initiated at 3×10^5 cells/ml either as monolayer cultures in T-25 flasks or on microcarrier beads at 15 cells/bead in either static (in 35-mm petri dishes) or dynamic (low shear stress RWV cultures) 3D cultures. Cells grew well in all three conditions with the monolayer cultures plateauing at Day 8 (Fig. 1). The petri and RWV cultures continued to proliferate the full 14 d. Doubling times during the first 8 d averaged 45.8, 56.1, and 52.3 h for the Petri, RWV, and T-25 cultures, respectively. Viability was 95% or greater at each time point by trypan blue dye exclusion. Although monolayer cultures remained predominantly as monolayers at least through 8 d (Fig. 2 A), both the static (Fig. 2 B) and dynamic (Fig. 2 C) cultures produced multilayer cell cultures indicating 3D growth. After 8 d, the monolayer cultures began to pile up and were no longer strictly monolayers. Thus, all three conditions led to growth of viable MIP-101 cells, although the monolayer culture entered a plateau phase by 8 d that was not apparent in either the static or dynamic 3D culture system.

Detection of CEA in the cytoplasm of 3D MIP-101 cultures. Monolayer and 3D cultures of MIP-101 cells were harvested and analyzed for expression of CEA-related proteins by immunohistochemistry. Monolayer cultures in the exponential phase did not react with the anti-CEA monoclonal antibody (Fig. 3). While trace expression of CEA-related proteins was evident by Day 4 in the RWV cultures.

① AU: 8 LMS 01? SAME LOCATION.

② AU: SPELL OUT 1ST TIME USED.

③ AU: SPELL OUT 1ST TIME USED.

④ AU: 228.2 is NAME OF MURINE I9G?

⑤ AU: SPELL OUT FIRST TIME.

⑥ AU: SPELL OUT FIRST TIME USED.

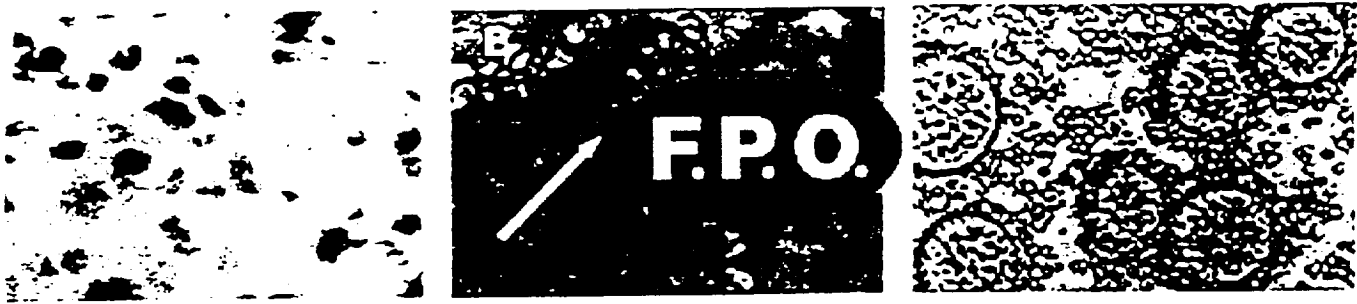


FIG. 2. Pattern of growth under different conditions. MIP-101 cells were cultured as monolayers in T-25 flasks (A), in static 3D cultures on microcarrier beads in nonstick petri dishes (B), or in dynamic 3D cultures in the rotating wall vessel (RWV) (C). MIP-101 cells form multilayer structures on microcarrier beads in both petri and RWV cultures. A and B are at $\times 40$, whereas C is at $\times 10$. Arrow in B denotes the edge of the microcarrier bead.

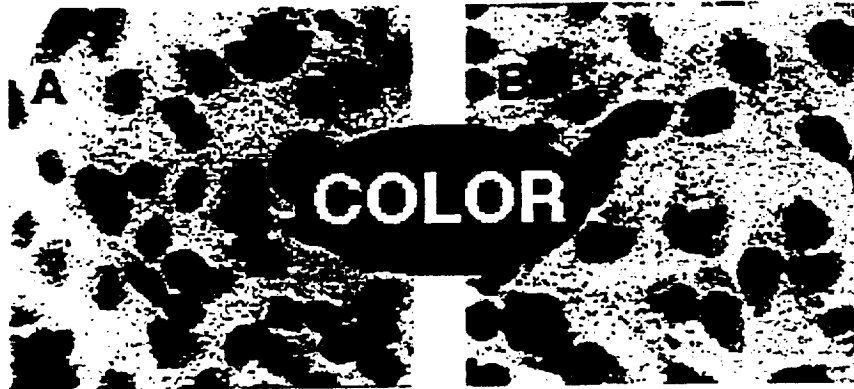


FIG. 3. Immunohistochemistry of MIP-101 cells growing as monolayers. MIP-101 cells were cultured for 6 d in T-25 flasks and then incubated without primary anti-carcinoembryonic antigen (CEA) antibody (A) or with an anti-CEA monoclonal antibody (B). After completion of staining as described in "Materials and Methods," CEA was not detected in MIP-101 cells. Magnification = $\times 60$.

the expression increased in 8- and 14-d cultures (Fig. 4 A–C). Cultures in the petri dishes were similar, although slightly less intense at each time point (Fig. 4 D–F). Expression was localized in the cytoplasm and was not present in plasma membranes of MIP-101 cells (Fig. 4 C and F).

Identification of CEA and NCA proteins in MIP-101 cultures. Because the immunohistochemical analysis may identify either 180 kDa CEA or 50 or 90 kDa NCA, we sought to determine which CEA-related proteins are expressed in MIP-101 cells grown under the different conditions. Western blots of extracts of MIP-101 cells were probed with monoclonal antibodies directed to NCA or CEA. Extracts of MIP-101 cells growing exponentially in monolayer culture displayed small amounts of CEA and both 50 and 90 kDa NCA proteins (Fig. 5 A and B). However, extracts of either the petri or RWV 3D cultures grown for 12 d expressed increased amounts of both 180 kDa CEA and the 50 kDa NCA proteins (Fig. 5 A and B). When densitometry was performed and the amounts of proteins compared to standards of partially purified CEA or NCA (data not shown), the amount of 180 kDa CEA was increased 6.2-fold in the petri culture and 4.2–7.4 in the RWV cultures. It is not clear why one of the RWV cultures did not produce CEA, although it clearly contained NCA (Fig. 5 A and B). Although the amount of 90 kDa NCA was not increased significantly in the 3D cultures (ratios of RWV:monolayer culture extracts of 90 kDa NCA were only 0.9–2.4, while the petri

dish ratio was 1.2), the amount of 50 kDa NCA was significantly increased in the 3D cultures (9.4-fold in the petri dish culture and 3.8–10.0-fold in the RWV cultures compared to the amount in the monolayer cell cultures). This demonstrates that MIP-101 cells grown in a 3D culture system produce increased amounts of mature CEA and NCA proteins with a relatively greater increase in the amount of 50 kDa NCA.

DISCUSSION

CEA functions *in vitro* as an intercellular adhesion molecule since it causes homotypic cell aggregation when transfected into cells that do not aggregate otherwise (1,20). Human colorectal carcinoma cells (13,15) and normal colon epithelial cells (10) also adhere to CEA attached to a solid phase through homophilic bonds. However, a role for CEA as an adhesion molecule *in vivo* has been difficult to define. CEA stimulates experimental and, possibly, clinical metastasis by a mechanism that does not involve cell adhesion because systemic pretreatment increases hepatic sequestration of weakly metastatic non-CEA expressing lines. Thus, CEA increases metastatic potential by some humoral effect that enhances sequestration of tumor cells in the liver.

We now report that 3D growth stimulates expression of CEA-related proteins in MIP-101 cells. Previous reports have shown that

①

① AU: "... IN THE AMOUNT OF NCA."?

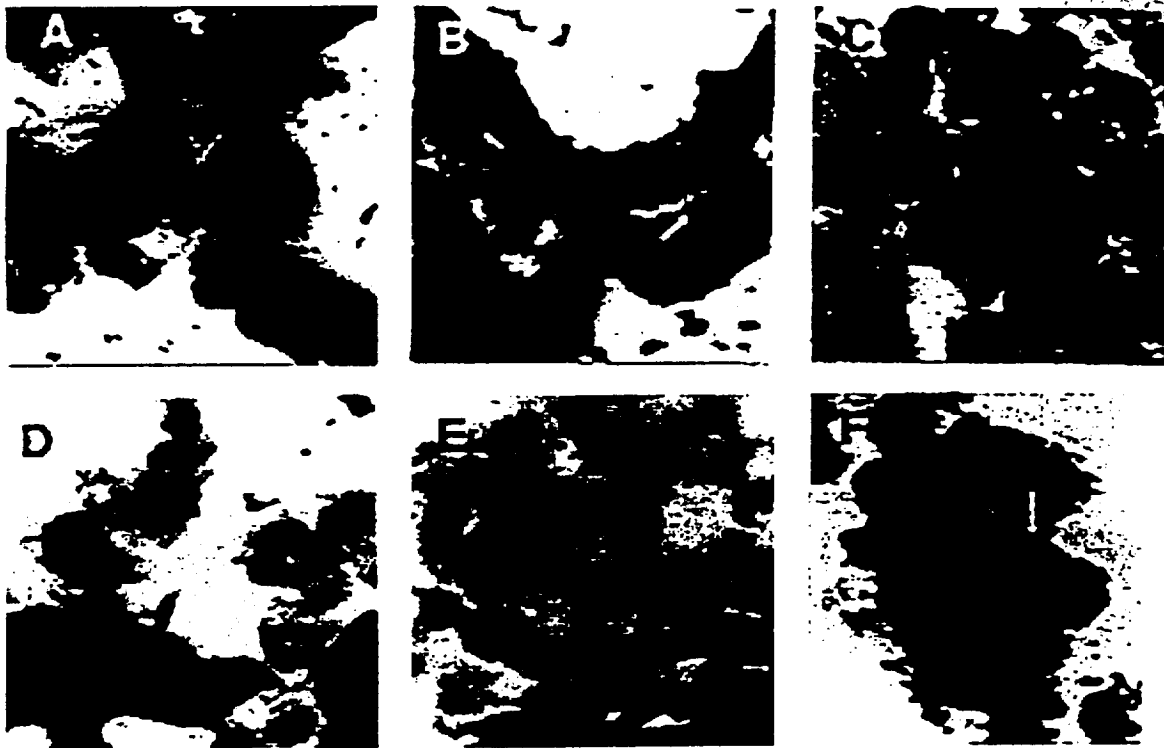


FIG. 4. Detection of carcinoembryonic antigen (CEA) in 3D CEA cultures. MIP-101 cells were grown on microcarrier beads in either the rotating wall vessel (RWV) (A-C) or in static microcarrier cultures in nonadherent petri dishes (D-F). On Days 4 (A,D), 8 (B,E), or 14 (C,F), cultures were harvested, fixed, and processed for CEA immunohistochemistry. CEA expression was not evident at 4 d in either RWV (A) or petri (D) cultures. However, CEA expression was evident at Day 8 (arrows, B and E) and increased at Day 14 in the Petri culture (F) but even more in the RWV culture (C). CEA is localized in the cytoplasm and does not mark intercellular boundaries as would be expected if it were present in the cell membrane. Magnification = $\times 60$.

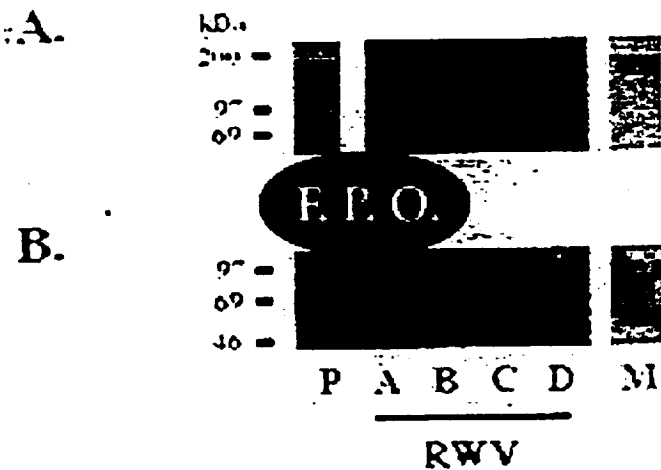


FIG. 5. Western blots of carcinoembryonic antigen (CEA) (A) and non-specific cross-reacting antigen (NCA) (B) expression in MIP-101 cells cultured under different conditions. MIP-101 cells were grown either in monolayer cultures (M), on microcarrier beads in nonadherent petri dishes (P), or in the rotating wall vessel (RWV) (A-D). 10^7 cells were extracted and analyzed for the content of 180 kDa CEA (A) or 50 and 90 kDa NCA (B). The results indicate that the expression of both CEA and NCA proteins is increased in 3D cultures of MIP-101.

expression of CEA is increased by differentiation agents and cytokines (18), as well as interferons (24). It is possible that 3D growth stimulates the production of transcription factors that may also be activated by cytokines. Clearly, further work is necessary to determine whether the regulation of CEA and NCA 50/90 occurs at the transcriptional, posttranscriptional, or translational level.

The expression of CEA-related proteins in MIP-101 in 3D culture is relatively weak and confined to the cytoplasm. CEA and NCA are bound to the plasma membrane through a glycosylphosphatidylinositol (GPI)-linkage (23). Release of CEA from cells may occur by cleavage of the GPI-linkage by an endogenous phosphatidylinositol-specific phospholipase (9). Because MIP-101 cells do not appear to localize CEA-related proteins to the plasma membrane, they may lack the ability to form the appropriate GPI-linkage. This may also explain why little CEA is released into the medium in cultures with high viability and low shear stress, since CEA may not be released from viable cells if it is not attached to the cell surface. An earlier report suggested that CEA was released by MIP-101 cells into the medium (12), but this may have reflected cell lysis in initial experiments in the RWV with higher shear stress from more turbulent conditions. The elevated blood levels of nude mice bearing intra-peritoneal MIP-101 may reflect the lysis of tumor cells as tumor growth outstrips blood supply (14) rather than secretion of CEA from viable cells.

Production of CEA-related proteins appears to be greater in the RWV than in the static nonstick petri dish culture. The RWV may provide better nutrient mixing than the static culture since the rotation provides some mixture of microcarrier bead aggregates through the medium, whereas the static system depends on simple diffusion for nutrient transfer. Further work is necessary to determine whether other metabolic effects are altering gene expression, since RWV cultures have similar glucose and oxygen consumptions as monolayer cultures do, but produce more hydrogen ion and carbon dioxide on a per cell basis (data not shown). This observation may suggest that anaerobic metabolism is increased in the RWV and that this is associated with the expression of CEA by MIP-101 cells.

Our present data suggest that the greatest increase in expression of CEA-related proteins occurs in the expression of 50 kDa NCA, followed by smaller increases in the expression of 180 kDa CEA without much change in the expression of 90 kDa NCA. The relatively greater increase in NCA expression is consistent with the relative increases that occur in NCA and CEA expression by human bowel epithelium during neoplastic progression. As normal colon epithelium becomes malignant, the relative expression of NCA also increases more than the increase in CEA expression (2). Since both 50 and 90 kDa NCA have the same peptide but different degrees of glycosylation, the present results suggest that production of the peptide may be increased but that posttranslational modification by increased glycosylation does not follow in parallel.

In summary, CEA is associated with the development of metastasis by human colorectal carcinoma. To the best of our knowledge, this is the first observation that 3D culture induces expression of CEA. Whether CEA or NCA expression is merely associated with or causes metastasis remains to be elucidated and was not evaluated in these experiments. Nonetheless, CEA expression is a marker of metastatic potential in MIP-101 cells. Future studies will seek to elucidate the mechanism by which 3D growth induces expression of CEA-related proteins. In addition, these experiments support the use of 3D culture techniques to investigate host-tumor interactions. Clearly, orthotopic implantation into the peritoneum of nude mice permits CEA expression, but may not actively stimulate it. Conversely, the subcutaneous tissue of nude mice must actively inhibit CEA expression that would otherwise occur in a 3D nodule. Similar differences in the metastatic behavior of human colon carcinomas have been noted by Fidler and colleagues (3,16), who suggest that the environment that is similar anatomically to the original site in which the cancer arose or metastasizes (the orthotopic site) induces production of proteases and other molecules that facilitate metastasis, whereas the subcutaneous tissue inhibits the expression of these molecules and inhibits metastasis. Thus, 3D growth may regulate gene expression that is not evident in monolayer cultures and that is further modulated in the host micro-environment.

ACKNOWLEDGMENTS

Supported by Grants NAC9-520 and NAC9-650 from the National Aeronautics and Space Administration and R01 CA 42857 from the Department of Health and Human Services.

REFERENCES

1. Benchimol, S.; Fuks, A.; Jothy, S., et al. Carcinoembryonic antigen, a human tumor marker, functions as an intercellular adhesion molecule. *Cell* 57:327-334; 1989.

2. Chu, K. F.; Jessup, J. M.; Frazier, M. L. Proliminant expression of mRNA coding for nonspecific cross-reacting antigen in colorectal carcinomas. *Tumor Biol.* 12:298-308; 1991.

3. Fidler, I. J. Orthotopic implantation of human colon carcinomas into nude mice provides a valuable model for the biology and therapy of metastasis. *Cancer Metastasis Rev.* 10:229-243; 1991.

4. Giavazzi, R.; Campbell, D. E.; Jessup, J. M., et al. Metastatic behavior of tumor cells isolated from primary and metastatic human colorectal carcinomas implanted into different sites in nude mice. *Cancer Res.* 46:1928-1933; 1986.

5. Goodwin, T. J.; Jessup, J. M.; Wolf, D. A. Morphological differentiation of human colorectal carcinoma in rotating wall vessels. *In Vitro Cell. Dev. Biol.* 28A:47-60; 1992.

6. Goodwin, T. J.; Schroeder, W. F.; Wolf, D. A., et al. Rotating-wall vessel coculture of small intestine as a prelude to tissue modeling: aspects of simulated microgravity. *Proc. Soc. Exp. Biol. Med.* 202:181-92; 1993.

7. Goslin, R.; Steele, G., Jr.; MacIntyre, J., et al. The use of preoperative plasma CEA levels for the stratification of patients after curative resection of colorectal cancers. *Ann. Surg.* 192:747-751; 1980.

8. Graham, C. H.; Kobayashi, H.; Stankiewicz, K. S., et al. Rapid acquisition of multicellular drug resistance after a single exposure of mammary tumor cells to antitumor alkylating agents. *J. Natl. Cancer Inst.* 86:975-982; 1994.

9. Hefta, S.; Hefta, L.; Lee, T., et al. Carcinoembryonic antigen is anchored to membranes by covalent attachment to a glycosylphosphatidylinositol moiety: identification of the ethanolamine linkage site. *Proc. Natl. Acad. Sci. USA* 85:4648-4652; 1988.

10. Ishii, S.; Ford, R.; Thomas, P., et al. CD44 participates in the adhesion of human colorectal carcinoma cells to laminin and type IV collagen. *Surg. Oncol.* 2:255-264; 1993.

11. Jessup, J. M.; Giavazzi, R.; Campbell, D., et al. Metastatic potential of human colorectal carcinomas implanted into nude mice: prediction of clinical outcome in patients operated upon for cure. *Cancer Res.* 49:6906-6910; 1989.

12. Jessup, J. M.; Goodwin, T. J.; Spaulding, G. Prospects for use of microgravity-based bioreactors to study three-dimensional host-tumor interactions in human neoplasia. *J. Cell. Biochem.* 51:290-300; 1993.

13. Jessup, J. M.; Kim, J. C.; Thomas, P., et al. Adhesion to carcinoembryonic antigen by human colorectal carcinoma cells involves at least two epitopes. *Int. J. Cancer* 55:262-268; 1993.

14. Jessup, J. M.; Petrick, A. T.; Toth, C. A., et al. Carcinoembryonic antigen: enhancement of liver colonisation through retention of human colorectal carcinoma cells. *Br. J. Cancer* 67:464-470; 1993.

15. Levin, L. V.; Griffin, T. W. Specific adhesion of carcinoembryonic antigen-bearing colorectal cancer cells to immobilized carcinoembryonic antigen. *Cancer Lett.* 60:143-152; 1991.

16. Morikawa, K.; Walker, S. M.; Nakajima, M., et al. Influence of organ environment on the growth, selection, and metastasis of human colon carcinoma cells in nude mice. *Cancer Res.* 48:6863-6871; 1988.

17. Niles, R. M.; Wilhelm, S. A.; Steele, G. D., et al. Isolation and characterization of an undifferentiated human colon cancer cell line (MIP-101). *Cancer Invest.* 5:545-552; 1987.

18. Niles, R. M.; Wilhelm, S. A.; Thomas, P., et al. The effect of sodium butyrate and retinoic acid on growth and CEA production in a series of human colorectal tumor cell lines representing different states of differentiation. *Cancer Invest.* 6:39-45; 1988.

19. Oikawa, S.; Imajo, S.; Noguchi, T., et al. The carcinoembryonic antigen (CEA) contains multiple immunoglobulin-like domains. *Biochem. Biophys. Res. Commun.* 144:634-642; 1987.

20. Oikawa, S.; Inezuka, C.; Kwoki, M., et al. Cell adhesion activity of non-specific cross-reacting antigen (NCA) and carcinoembryonic antigen (CEA) expressed on CHO cell surface, homophilic and heterophilic adhesion. *Biochem. Biophys. Res. Comm.* 164:39-48; 1989.

21. Paget, S. The distribution of secondary growths in cancer of the breast. *Lancet* i:571-573; 1889.

22. Rak, J. W.; Kerbel, R. S. Growth advantage ("clonal dominance") of metastatically competent tumor cell variants expressed under selective two- or three-dimensional tissue culture conditions. *In Vitro Cell. Dev. Biol.* 29A:742-748; 1993.

[Handwritten signature]

① AU: WHAT IS "i" 1989 - it is volume i for year 1989
 ② AU: JOURNAL CORRECT? - Yes.
 ③ AU: JOURNAL NOT IN MY SOURCE - [unclear] was published by [unclear]

- Muster*
23. Sack, T.; Gum, J.; Low, M., et al. Release of carcinoembryonic antigen from human colon cancer cells by phosphoinositol-specific phospholipase C. *J. Clin. Invest.* 82:586-593; 1988.
 24. Takahashi, H.; Okai, Y.; Paxton, R. J., et al. Differential regulation of carcinoembryonic antigen and biliary glycoprotein by gamma-interferon. *Cancer Res.* 53:1612-9; 1993.
 25. Tibbetts, L. M.; Doremus, C. M.; Tzanakakis, G. N., et al. Liver metastases with 10 human colon carcinoma cell lines in nude mice and association with carcinoembryonic antigen production. *Cancer* 71:315-321; 1993.
 26. Wagner, H. E.; Thomas, P.; Wolf, B. C., et al. Characterization of the tumorigenic and metastatic potential of a poorly differentiated human colon cancer cell line. *Invasion & Metastasis* 10:253-266; 1990.
 27. Wanebo, H. J.; Rao, B.; Pinsky, C. M., et al. Preoperative carcinoembryonic antigen level as a prognostic indicator in colorectal cancer. *N. Engl. J. Med.* 299:448-451; 1978.
 28. Wilmanns, C.; Fan, D.; O'Brian, C. A., et al. Orthotopic and ectopic organ environments differentially influence the sensitivity of murine colon carcinoma cells to doxorubicin and 5-fluorouracil. *Int. J. Cancer* 52:98-104; 1992.

① Au: pg RANGE 1619? -/yes.

Implantation of human colorectal carcinoma cells in the liver studied by *in vivo* fluorescence videomicroscopy

Seiichi Ishii, Takayuki Mizoi, Katsunori Kawano*, Osman Cay*, Peter Thomas, Alexander Nachman, Rosilyn Ford, Yutaka Shoji, John B. Kruskal*, Glenn Steele Jr and J. Milburn Jessup

Laboratory of Cancer Biology, Department of Surgery; and *Department of Radiological Sciences, New England Deaconess Hospital, Harvard Medical School, Boston, MA, USA

(Received 22 May 1995; accepted in revised form 27 November 1995)

In vivo fluorescence videomicroscopy (IVFM) was used to analyse the behavior of weakly and highly metastatic human colorectal carcinoma (CRC) cells during implantation in the liver. A highly metastatic human CRC cell line, CX-1, and a weakly metastatic line, Clone A, were double-labeled with rhodamine B isothiocyanate-dextran (Rd-Dx) to locate cells and with calcein AM to assess cell metabolic activity in an experimental metastasis model. Double-labeled CRC cells (2.0×10^6) were injected into the spleens of groups of nude mice and the livers observed by IVFM over the next 72 h. CRC cells were implanted within 30 s after injection into either portal venules or the proximal third of hepatic sinusoids. Approximately 0.5% of CRC cells traversed the liver through portal-central venous shunts and implanted in the lung. The number of CX-1 cells in the liver was similar to that of Clone A cells during the first 12 h. However, more CX-1 cells than Clone A cells remained in the liver at 24 h and were in groups of 8–12 cells whereas only a few, single Clone A cells were detected in the liver at 72 h. Not all Clone A cells are committed to die within 4 h of implantation because cells harvested 4 h after hepatic implantation proliferated normally *in vitro* when removed from the hepatic microenvironment. Since the stress of mechanical deformation during implantation may cause differences in cell survival, CX-1 and Clone A cells were passed through filters with 8 μm pores *in vitro* at 10–15 cm of water pressure to recreate the trauma of hepatic implantation. Approximately 50% of both CX-1 and Clone A cells were lysed. Furthermore, both CRC lines remained metabolically active when co-cultivated with liver cells for at least 24 h *in vitro*. Thus, the difference in metastatic potential between the two CRC lines may reside in their response to the combination of mechanical implantation and subsequent growth in the liver parenchyma.

Keywords: hepatic sinusoids, intravital microscopy, micrometastasis

Introduction

The liver is the most common site of visceral metastasis by human colorectal carcinoma. Unlike other malignant neoplasms, some patients with hepatic metastases are amenable to resection with survival rates of 25–30% [1,2] because the original metastases do not produce secondary metastases. What determines either the number or pattern of hepatic metastases is

not fully understood. One approach to this problem is to analyse how colorectal carcinoma (CRC) behave during the early events of implantation within the liver in an *in vivo* model of experimental hepatic metastasis in athymic nude mice.

Experimental hepatic metastasis following the intrasplenic injection of human CRC cells is a good model for the analysis of the implantation of metastasis because: (a) the ability of human CRC to develop liver colonies after intrasplenic injection (i.e. 'metastatic potential') is associated with the development of metastases in patients [3], (b) the number of

Address correspondence to: J. M. Jessup, Department of Surgery, Deaconess Hospital, 110 Francis Street Suite 3-A, Boston, MA 02215, USA. Fax: (+1) 617 632 7424.

[¹²⁵I]IdUrd-prelabeled CRC cells remaining in the liver 4–24 h after intrasplenic injection is associated with the subsequent appearance of liver colonies [4], and (c) metastatic potential is directly associated with the number of CRC cells surviving 4 h in the liver [5]. Highly metastatic human CRC are those lines that produce liver colonies in more than 50% of athymic nude mice within 60 days after the intrasplenic injection of 2×10^6 viable tumor cells while weakly metastatic CRC produce liver colonies in 20% or fewer mice under the same conditions [5]. Weiss *et al.* [6], Barbera-Guillem *et al.* [7,8] and others [9–11] have demonstrated that metastasis to the liver results from a series of linked steps in which metastatic precursor cells lodge in the hepatic parenchyma, extravasate across the endothelium, and then proliferate within the parenchyma. During this inefficient process, metastatic precursor cells may die because (a) cells undergo deformation injury and lyse during implantation, (b) they do not adhere to endothelial or other cells lining the microvasculature, (c) they do not migrate across the endothelium, or (d) they cannot proliferate once they reach the parenchyma, possibly because cytotoxic host cells (e.g. Kupffer and pit cells) kill them. Since our data support the hypothesis that metastatic potential is directly associated with surviving the initial implantation, our aim was to identify whether highly and weakly metastatic CRC behaved differently during the initial implantation and migration into the hepatic parenchyma.

For this purpose, we used *in vivo* fluorescence microscopy (IVFM) to directly observe the implantation of CRC cells within the hepatic microvasculature. Burkart and Friedrich [12] originally applied *in vivo* videomicroscopy to observe that Kupffer and hepatic endothelial cells interact with circulating erythrocytes and leukemia cells during experimental hepatic metastasis. Labeling cells with fluorescent probes facilitates the visualization of carcinoma cells *in vivo* so that cell viability and location may be assessed. However, the choice of fluorescent marker may influence the outcome of the study. Weiss *et al.* [6] observed that sarcoma cells labeled with acridine orange were lethally deformed in the microcirculation of cremaster muscles within several minutes after implantation. Since acridine orange loses intense fluorescence within 30 min [6] and interferes with DNA replication and transcription [13], it can only be used to assess the earliest phases of implantation. Calcein AM, a non-toxic membrane-permeable fluorescing reagent, is a better probe for the initial phases of implantation because it only produces strong fluorescence in live cells with cytoplasmic esterase activity [14] and does not alter the

deformation resistance of cells [15]. However, the disadvantage of calcein AM is that it diffuses so quickly out of cells that not enough is present intracellularly to be a useful marker after 48 h. Nonetheless, calcein AM has been used successfully to study the arrest and extravasation of melanoma cells through the chorioallantoic membrane for 26 h [16,17]. Thus, other techniques must be used for long-term visualization of carcinoma metastasis *in vivo*. While Morris *et al.* [18] labeled cells with small (0.2 μ m) fluorescent beads that are retained in tumor cells, we explored the use of rhodamine-conjugated low molecular weight dextran (Rd-Dx) that was scrape-loaded into CRC cells. Rd-Dx is non-toxic, does not leach out of cell cytoplasm, and retains its fluorescence until diluted by cell division. Rd-Dx is concentrated enough to be detectable for 7 days within the cytoplasm of CRC cells proliferating *in vitro* or implanted in the livers of nude mice. Thus, Rd-Dx marks the number and location of CRC cells while calcein AM identifies metabolically active cells during the first 24 h after implantation.

Combining this double-labeling technique with IVFM, we examined the early fate of two CRC lines with different metastatic potentials in the hepatic microcirculation. Further, we tested the effect of simple mechanical stress on CRC cells as a possible cause of CRC cell death in the liver using an *in vitro* model that resembles the physical parameters of the sinusoidal microenvironment. We also assessed the ability of each CRC line to survive for 24 h when co-cultivated *in vitro* with murine hepatic cells. Our data suggest that the difference in metastatic potential for each CRC cell line is due to different capacities to proliferate within the hepatic parenchyma after mechanical implantation.

Materials and methods

Human colorectal carcinoma cell lines

A poorly differentiated human CRC line, Clone A, was obtained from D. L. Dexter (DuPont DeNemours & Co., Wilmington, DE, USA) and is weakly metastatic since it produces liver colonies in 8% of nude mice injected with 2×10^6 cells intrasplenically [5]. CX-1, a moderately to well-differentiated human CRC line, is a highly metastatic CRC line that produces liver colonies in 93% of nude mice after intrasplenic injection [5] and was derived from the HT-29 cell line and provided by Dr L. B. Chen (Dana-Farber Cancer Institute, Boston, MA, USA). The two CRC lines were maintained in RPMI 1640 medium (Gibco Laboratories Life Technologies Inc., Grand Island, NY, USA) with 10% fetal bovine serum (FBS; Sigma Chemical Company, St Louis, MO, USA), 1% L-glutamine (Gibco), 100

units/ml of penicillin G (Gibco) and 100 mg/ml of streptomycin (Gibco). Both CRC lines were checked frequently for the presence of mycoplasma by Hoechst 33258 staining as well as by Gen-Probe (Gen-Probe, Inc., San Diego, CA, USA) and were negative.

Cell labeling

To visualize carcinoma cells by fluorescence microscopy, CRC cells were labeled with two fluorescing reagents, rhodamine B isothiocyanate-dextran (Rd-Dx; Sigma) with a maximum excitation/emission at 530/590 nm and calcein AM (Molecular Probes Inc., Eugene, OR, USA) with a maximum excitation/emission at 485/530 nm. Rd-Dx was first incorporated into CRC cells using a modification of the scrape-loading technique described by McNeil *et al.* [19] and McNeil [20]. CRC cells (90% confluent) in 150 mm tissue culture dishes (Corning Inc., Corning, NY, USA) were washed with divalent cation-free PBS warmed to 37°C (Gibco), and covered with 2.0 ml/dish of 10 mg/ml Rd-Dx in PBS. Cells were then scraped with a scraper (Costar, Cambridge, MA, USA) to load the Rd-Dx and washed twice with PBS. The Rd-Dx loaded cells were incubated for 16 h at 37°C in complete tissue culture medium and then adherent cells were recovered by trypsin (Gibco). The cells were suspended at 1.0×10^7 cells/ml in PBS and incubated with calcein AM at a final concentration of 4 μ M for 30 min at 37°C. After washing twice with PBS, the cells were suspended in PBS at 2.0×10^7 cells/ml and were used for the IVFM study. At least 90% of the cells were labeled with both fluorescent markers in each experiment. Cells were also tested for viability by staining with trypan blue vital dye (Gibco).

Animals

Six-week-old BALB/c athymic mice weighing 20–25 g were obtained from Harlan Sprague-Dawley Inc. (Indianapolis, IN, USA) and were kept under pathogen-free conditions. Tumor cell injection and IVFM were performed under general anesthesia with intraperitoneal administration of pentobarbital (50 mg/kg) (Abbott Laboratories, North Chicago, IL, USA). All animal experiments were approved by the Animal Care and Use Committee of the Deaconess Hospital and were conducted in accordance with the guidelines issued by the National Institutes of Health for care of laboratory animals.

In vivo fluorescence videomicroscopy

The double-labeled CRC cells (2.0×10^6) suspended in 0.1 ml of PBS were injected into the spleens of each mouse. The number and localization of CRC cells in the murine livers were directly observed and recorded

by IVFM at 0–30 min, 4 h, 12 h, 24 h and 72 h after intrasplenic injection of groups of two mice at each time point. Three mice were kept alive for 38 days after intrasplenic injection of the double-labeled CRC cells and examined for the development of hepatic colonies.

IVFM was performed following the methods described by Post *et al.* [21] and Kawano *et al.* [22]. Briefly, the left lateral hepatic lobe was gently exteriorized through an upper horizontal incision under general anesthesia and was placed on a quartz crystal stage designed for *in vivo* microscopy. The exposed liver was covered with a piece of wet Saran Wrap (Dow Chemical, Midland, MI, USA) to avoid desiccation. CRC cells in the liver were then observed with a microscope (Optiphot, Nikon Co., Tokyo, Japan, USA) equipped with water-immersion objectives ($10 \times$ – $40 \times$), a zoom lens and epi-fluorescence. An epi-fluorescence filter with a combination of 510–560 nm and > 580 nm for excitation and emission (G-1B, Nikon) was used to visualize Rd-Dx while a filter with a combination of 450–490 nm/ > 515 nm for excitation/emission (B-2E, Nikon) was used for calcein AM visualization. Dynamic images of CRC cells in the liver were recorded on S-VHS videotape with a video camera (CCD72; Dage-MTI Inc., Michigan City, IL, USA) and S-VHS tape recorder (AG-1830; Panasonic, Osaka, Japan) connected to the microscope. Eight to ten fields per mouse were observed and recorded at $100 \times$ for 15 s/field for each fluorescence channel. The fields were selected along the margins of the lateral segment of the left lobe and included a portal branch in the center of each field. The number and location of CRC cells in the liver were examined during off-line analysis of the video-recorded images. Each fluorescing spot in the liver appeared to be one CRC cell. The number of cells in the liver was enumerated per square millimeter of the liver (cells/mm²). Viability of the CRC cells in the liver was calculated by dividing the number of calcein AM positive cells by the number of Rd-Dx positive cells within the same image. Still pictures of IVFM images were taken through a camera (FE, Nikon) connected to the microscope with ISO 400 film. Also in some experiments mice were sacrificed and then the lungs were examined by IVFM.

Histological studies

After observation by IVFM, the mice were sacrificed and the livers were fixed with 10% formalin or 1.5% glutaraldehyde in PBS. Three to five sections per liver were examined histologically by H&E staining. To identify CX-1 cells in the liver, immunohistochemical staining of carcinoembryonic antigen (CEA) was performed with a murine anti-CEA IgG₁ monoclonal

antibody, A5B7 (DAKO Laboratories Inc., Denmark), since CX-1 cells strongly express CEA [23].

Isolation of CRC cells from the murine liver

To confirm the viability of poorly metastatic CRC cells in the liver, 2.0×10^6 of double-labeled Clone A cells were injected intrasplenically into a mouse whose liver was resected 4 h later, minced, and digested by trypsin (GIBCO) for 60 min at 37°C with gentle stirring. Digestion with trypsin was used to preferentially enrich tumor cells which are resistant to trypsinization by removing hepatic parenchymal and non-parenchymal cells. The tissue digest was suspended in PBS and single cells were recovered from the supernatant. Total numbers of viable isolated cells and fluorescing cells were counted by trypan blue and fluorescence microscopy. The cells were then cultured in complete tissue culture medium.

Co-culture of CRC with hepatic cells

The effect of hepatic cells on human CRC was studied in a novel *in vitro* co-culture system. Murine livers were perfused with PBS *in vivo* and removed after the mouse had been sacrificed by lethal injection. The livers were cut into 2–3 mm pieces and placed in a 50:50 mixture of hepatocyte growth medium (GIBCO) and complete tissue culture medium and cultured in a Rotating Wall Vessel (RWV; Synthecon, Inc., Houston, TX, USA) which is a 110 ml bioreactor that rotates cells around the horizontal axis under low shear stress [24]. Double-labeled CRC cells (2.0×10^6) were added and the mixture incubated at 37°C for 24 h. Two ml samples were taken at 0.16, 4, 8 and 24 h and the numbers of rhodamine- and calcein-labeled CRC cells determined on an inverted microscope equipped with epi-fluorescence (Diaphot, Nikon) using digital image capture by an Optronics integrating color CCD video camera (Model VI-470, Optronics Engineering, Goleta, CA, USA) and captured on a Macintosh Quadra 950 (Apple Computer Co., Cupertino, CA, USA) using Photoshop version 3.0 software (Adobe Systems Inc., Mountain View, CA, USA). Images were then processed and analysed as described for IVFM.

In vitro mechanical stress assay

The effect of mechanical stress on CRC cells was determined *in vitro* using a polycarbonate membrane with $8 \mu\text{m}$ pores (1×10^5 pores/ cm^2 , $7 \mu\text{m}$ in thickness; Costar). Fluorescence-labeled CRC cells (6×10^5) suspended in prewarmed Ringer's Injection USP (Baxter, Deerfield, IL, USA) were passed through the membrane by constant flow at a pressure of 15 cm H_2O . Fractions were collected every 30 s and centrifuged at $500 g$ for 5 min. Fluorescence intensity in

the pelleted cells was determined by a fluorescence concentration analyser (IDEXX Laboratories, Inc., Westbrook, ME, USA).

Statistical analysis

The results are expressed as mean \pm SEM of the number of fluorescing cells per field in the liver by IVFM with differences among groups of means tested by one-way analysis of variance (ANOVA). When ANOVA demonstrated that means within an experiment were significantly different from one another, significance between individual group means was tested with either the Fisher PLSD or Dunnett *t*-test with a significance level of 1%. All calculations were performed on a Macintosh microcomputer using Statview SE+ Graphics (Abacus Concepts, Inc., Berkeley, CA, USA).

Results

Effect of double-labeled CRC cells on growth potential
Clone A cells are slightly bigger than CX-1 cells with diameters of $18.24 \pm 0.59 \mu\text{m}$ and $14.28 \pm 0.48 \mu\text{m}$, respectively (mean \pm SEM). When double-labeled, more than 90% of the CRC cells had intense cytoplasmic staining for both Rd-Dx and calcein AM. The double-labeling did not alter the proliferation of Clone A cells cultured for at least 4 days *in vitro* (Figure 1). Similar results were obtained with CX-1 cells. Rd-Dx fluoresced for at least 4 days in the cytoplasm while calcein AM fluorescence was barely detectable after 24 h (data not shown). CRC cells implanting in murine livers were visualized clearly by IVFM with both

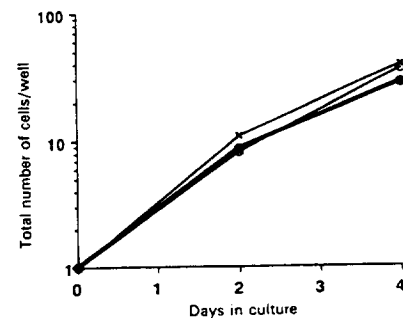


Figure 1. Clone A cells were loaded with Rd-Dx alone (x) or Rd-Dx and calcein AM (●) as described in Materials and methods and their capacity to proliferate *in vitro* compared to that of similar cells that had not been labeled with either compound (○). Neither fluorescent marker inhibited cell proliferation *in vitro*.

Figure 2. CX-1 cells trapped in the liver 10 min after intrasplenic injection. Phase contrast (A), Rd-Dx (B) and calcein AM (C) views of the same area. Portal venules (PV) can be seen on the phase contrast picture. CRC cells are clearly visualized by both Rd-Dx and calcein AM fluorescence.

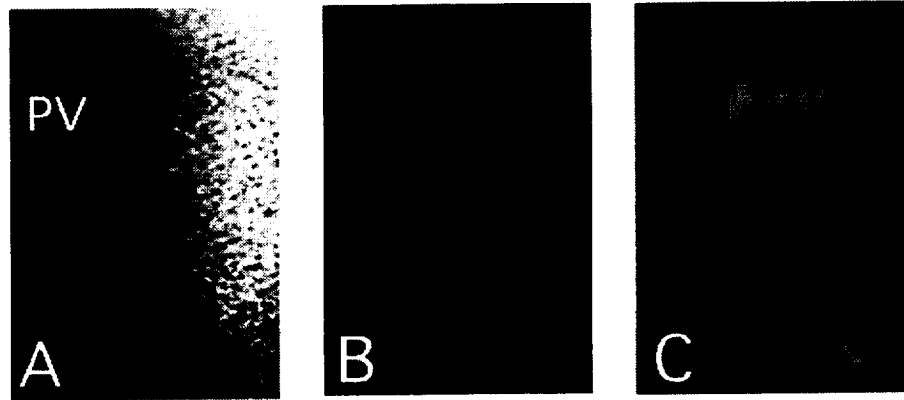
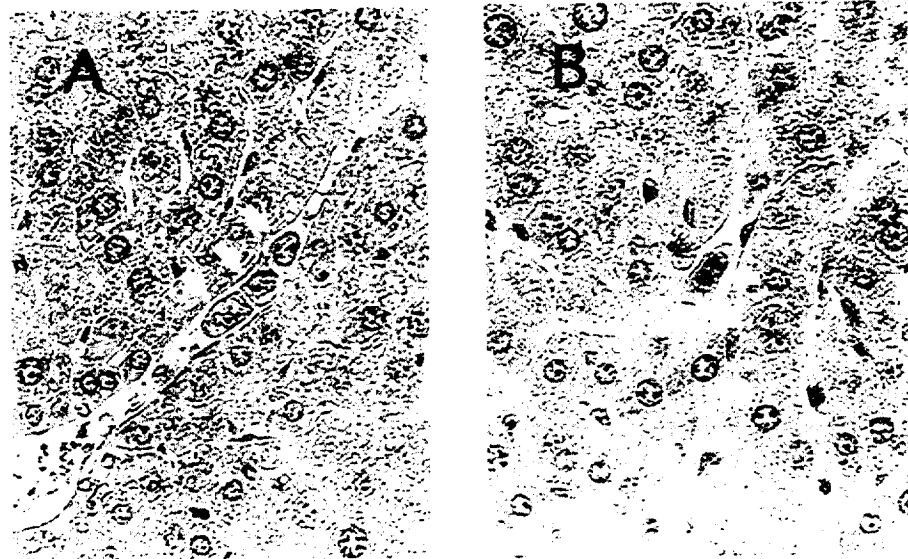


Figure 3. CX-1 (A) and Clone A (B) cells in the liver 30 min after intrasplenic injection. CRC cells (arrowheads) can be seen in the portal venules. Cells are elongated but lie within the vascular space. H&E.



Rd-Dx and calcein AM fluorescence during the first 24 h (Figure 2). Thus, the fluorescent dyes did not inhibit the capacity of CRC cells to proliferate and identified their entry into the liver.

IVFM of the initial implantation of CRC cells in the liver

CRC cells in the liver were directly observed by IVFM at 0–30 min, 4 h, 12 h, 24 h and 72 h after intrasplenic injection. Both CX-1 and Clone A cells appeared in the liver within 30 s after intrasplenic injection and implanted either as single cells or as doublets or triplets in single file in the terminal portal venules or in the proximal third of the sinusoids (Figure 2). This was confirmed by routine histology (Figure 3A, B). Although the spleen was left intact, CRC cells rarely implanted more than 5 min after injection. The majority of CRC cells were severely deformed within 4 h (Figure 4) and

began to lose calcein AM fluorescence (Figure 5). CX-1 cells did not extravasate into the hepatic parenchyma during the first 72 h but formed groups of 8–12 cells (data not shown).

Kinetics of survival after implantation

The kinetics of survival after implantation were different for CX-1 and Clone A cells during the first 72 h after intrasplenic injection. Although similar numbers of CX-1 and Clone A cells persisted in the liver during the first 12 h, the number of Rd-Dx-labeled CX-1 cells in the liver at 24 and 72 h was significantly greater than the number of Rd-Dx-labeled Clone A cells (Figure 6A). Significantly more calcein AM and Rd-Dx double-labeled CX-1 than Clone A cells were present in the hepatic sinusoid-portal venules 24 h after implantation (Figure 6B). These data suggest that more Clone A cells are removed from the liver than CX-1 cells during the first 24 h.

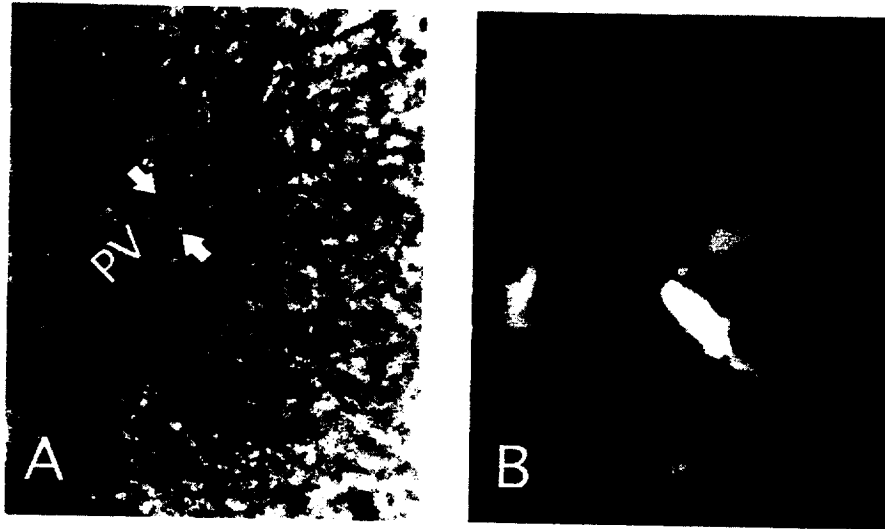


Figure 4. Deformity of Clone A cells in the periportal sinusoids at 4 h. Phase contrast (A) and Rd-Dx (B) views of the same area. Phase contrast view shows a portal venule (PV). Carcinoma cells in the periportal sinusoids show considerable deformity (B).

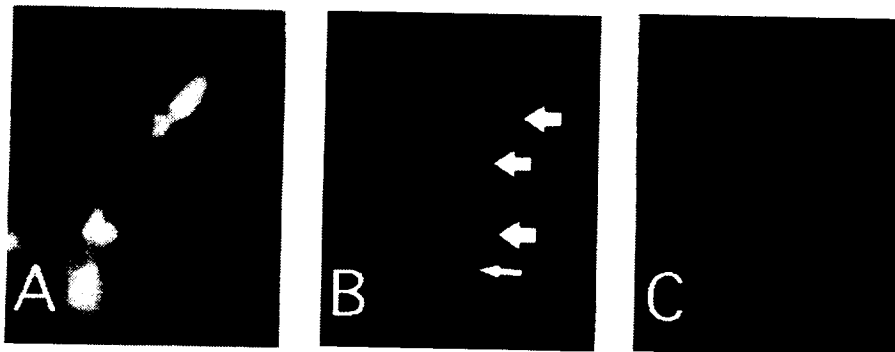


Figure 5. CX-1 cells in the liver losing calcein AM fluorescence at 4 h. Phase contrast + Rd-Dx (A), Rd-Dx (B) and calcein AM (C) views of the same area. CX-1 cells localize in the portal venule (pv) and periportal sinusoids in (A). The cells fluoresce intensely with Rd-Dx (B) but lose calcein fluorescence (C). Large arrows in (B) denote cells that are viable while the narrow arrow indicates cells that are not viable.

Detection of fewer calcein AM-stained Clone A cells within the liver at 24 h may reflect diffusion of dye from Clone A cells rather than cell lysis. To assess this, calcein AM and Rd-Dx double-labeled CRC cells were cultured in complete medium for 24 h and analysed for viability by trypan blue dye exclusion and for metabolic activity by fluorescent dye staining. Cells were at least 95% viable by trypan blue dye exclusion (Table 1). Approximately 70% of Rd-Dx-labeled Clone A and CX-1 cells also fluoresced with calcein AM (Table 1). In contrast, only 7% of double-labeled Clone A cells and 40% of double-labeled CX-1 cells fluoresced with calcein AM 24 h after hepatic implantation (Table 1). Thus, implantation in the liver decreases the proportion of calcein AM-metabolizing cells in both weakly and highly metastatic CRC, but has a greater effect on the weakly metastatic Clone A cell line.

Portal to central venous hepatic shunts in mice injected with CRC cells

Controversy exists about whether malignant cells may traverse the liver to gain access to other microcapillary beds. Four hours after injection abnormal portal vein to central venous shunts were observed in both CX-1- and Clone A-injected livers (Figure 7). When mice were sacrificed 4 h after intrasplenic injection and the lungs examined by IVFM to confirm whether CRC cells had traversed the liver, CRC cells were found in the lungs (data not shown). The percentage of CRC cells trapped in the lung was 0.5% or less for both CX-1- and Clone A-injected mice at 30 min and 4 h, which was determined with [¹²⁵I]IdUrd-labeled CRC cells (data not shown and [5]). Thus, the proportion of CRC cells that traverse the liver through these portal to central venous shunts is small but detectable.

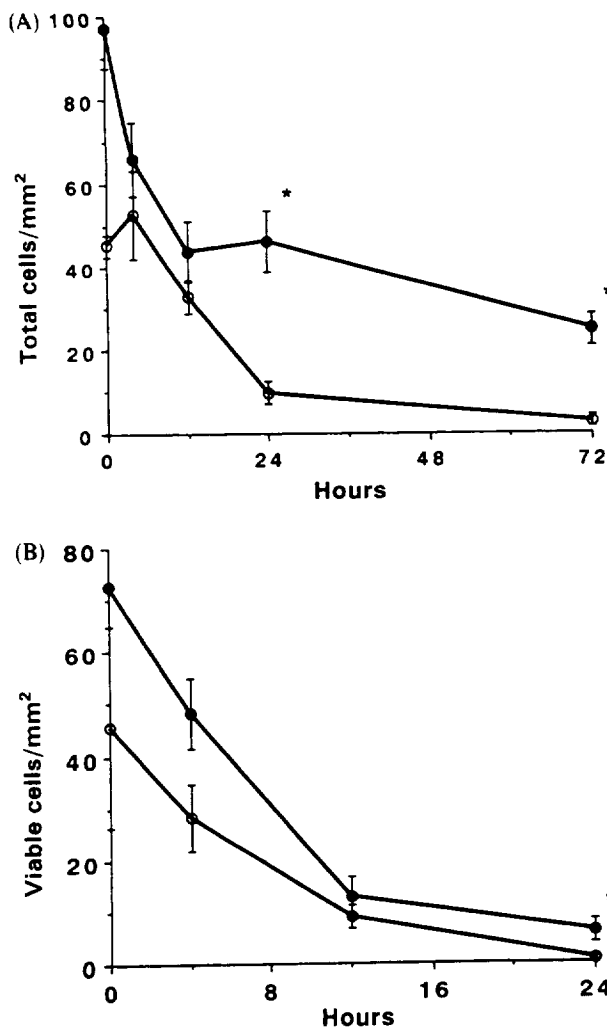


Figure 6. Kinetics of cell growth after hepatic implantation. The numbers of total (A) and viable (calcein AM-metabolizing) (B) CX-1 (●) and Clone A (○) cells were counted at the times indicated after intrasplenic injection and expressed as cells/mm². **P* < 0.01 by Student's *t*-test. Mean ± SEM are presented.

Recovery of Clone A cells from the liver

Since Clone A cells either died or stopped proliferating upon entry into the liver, they may be committed to die within the first 4 h after implantation in the liver. We tested this possibility by recovering Clone A cells 4 h after intrasplenic injection from the murine liver and preparing single cell suspensions by trypsin digestion. Cells (4–10%, 0.8–2 × 10⁵), that were positive for both Rd-Dx and calcein AM were isolated from livers in which 2 × 10⁶ double-labeled cells had been injected (Table 2). Three consecutive *in vivo* isolations of Clone A cells demonstrated that a significant fraction of Clone A cells harvested 4 h after

implantation proliferated if removed from the hepatic microenvironment (Table 2).

Effect of mechanical stress on CRC cells

To examine whether mechanical stress affected CRC cells differently, CX-1 and Clone A cells were tested in an *in vitro* assay that resembled the dimensions of the hepatic sinusoid. Both CX-1 and Clone A cells passed through the polycarbonate membrane within 2 min of the filtration with similar fractions of cells recovered after filtration (48.0% for CX-1 and 48.3% for Clone A with approximately 80% viability for each). Cultivation *in vitro* for 24 h did not result in any further loss of viability for either cell line (data not shown). Thus, both CRC cell lines appeared to be equally sensitive to the effects of mechanical deformation.

Effect of co-cultivation of CRC cells with murine hepatocytes

Although mechanical implantation may lyse approximately one-half of the cells entering the liver, other mechanisms must contribute to inhibit CRC proliferation in the liver parenchyma. One possible inhibitory

Table 1. Fluorescence staining of CRC cells 24 h after implantation in the liver

Condition	CRC line	% Metabolically active	<i>P</i>	% Viable
Liver implant	Clone A	3 ± 2		N.D.
Tissue culture	Clone A	71 ± 8	0.001	95 ± 2
Liver implant	CX-1	10 ± 3		N.D.
Tissue culture	CX-1	69 ± 7	0.001	98 ± 1

CRC cells were double-labeled with calcein AM and Rd-Dx (see Materials and methods) and either injected intrasplenicly to cause experimental hepatic metastasis (liver implant) or cultured in monolayer culture (tissue culture). Twenty-four hours later mice were either analysed by IVFM or the cultures were examined by epi-fluorescence. Results are expressed as mean ± SEM. % Metabolically active is the percentage of Rd-Dx-labeled CRC cells that also fluoresce with calcein AM. % Viable was determined in cultured cells by trypan blue dye exclusion.

%Metabolically active

$$= \frac{\text{No. of CRC cells + calcein AM}}{\text{No. of CRC cells + Rd-Dx}} \times 100$$

All values are percentages.

N.D. = not determined.

P values determined by two-tailed Student's *t*-test of the difference of the means of % Metabolically active for each CRC line.

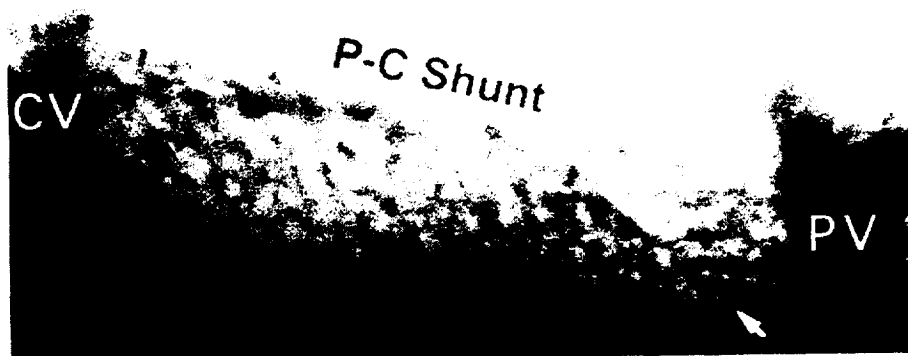


Figure 7. An abnormal portal to central venous shunt observed in the liver 4 h after CX-1 injection. Direction of blood flow from portal vein (PV) to central vein (CV) is indicated with arrows.

Table 2. Recovery of viable Clone A CRC cells 4 h after hepatic implantation

Experiment	No. of fluorescing Clone A cells recovered from murine liver	% of cells injected
1	2.0×10^5	10
2	0.8×10^5	4
3	0.8×10^5	4

Cells were isolated from murine liver by trypsin digestion 4 h after intrasplenic injection of 2.0×10^6 double-labeled Clone A cells. The isolated Clone A cells were expanded *in vitro* and re-injected intrasplenicly into a nude mouse. The *in vivo* isolation was repeated three times with an interval of approximately 4 weeks.

Fluorescing cells were calcein AM and Rd-Dx fluorescent cells.

% of cells injected is the number of Clone A cells recovered divided by the number of cells injected expressed as a percentage.

influence may be the hepatic cells themselves. Murine hepatic cells were cultured in a bioreactor for up to 10 days with good maintenance of tissue architecture (Figure 8A) and ability to metabolize calcein AM (Figure 8B,C). When the metabolic activity of double-labeled CRC cells in hepatic co-cultures was compared to that of CRC lines either cultured alone *in vitro* or after hepatic implantation *in vivo*, hepatic implantation was associated with a greater loss of calcein AM metabolizing activity than was simple culture *in vitro* or even co-culture with hepatic cells (Figure 9).

Discussion

The early phase of implantation and colonization was examined by IVFM with two CRC lines that have different metastatic potentials. CX-1 is a highly

metastatic CRC line producing hepatic colonies in 100% of nude mice by intrasplenic injection of 2×10^6 cells [24]. In contrast, Clone A produces liver colonies in less than 10% of nude mice after intrasplenic injection of the same number of CRC cells [5]. During the first 12 h after intrasplenic injection, both CRC cell lines implanted at similar sites with matching numbers of single, viable cells. However, more highly metastatic CX-1 cells were metabolically active in the liver after 24 h than weakly metastatic Clone A cells. The relationship between the number of viable CRC cells retained in the liver 4–24 h after implantation and the subsequent appearance of metastases was reported previously by Morikawa *et al.* [4] and Jessup *et al.* [5]. Weiss *et al.* [6], Barbera-Guillem *et al.* [7,8,25] and Morris *et al.* [18] have shown that the number of cells surviving the early implantation stresses of deformation, attachment and extravasation are similar between high and low metastatic cell lines. In addition, Morris *et al.* [18] have found that proliferation by metastatic precursor cells does not begin to occur within the hepatic parenchyma until 48 h after implantation. Since fewer double-labeled CRC cells were present after hepatic implantation than after either co-culture with hepatic cells or culture alone *in vitro*, the loss of calcein AM fluorescence by Rd-Dx-labeled cells reflects a decrease in metabolic activity rather than leakage of dye from the CRC cells. Thus, the present study extends these previous studies by showing that more highly metastatic CRC cells are alive in the liver 24 h after intrasplenic injection than weakly metastatic CRC. The surviving fraction of clonogenic metastatic precursor cells 24 h after implantation is around 5%.

CRC cells did not appear to migrate during the first 72 h after implantation. In addition, microscopic examination of the livers of nude mice demonstrated experimental metastases of CX-1 cells throughout the hepatic parenchyma (data not shown). In contrast, Morris *et al.* [18] have recently shown that metastatic

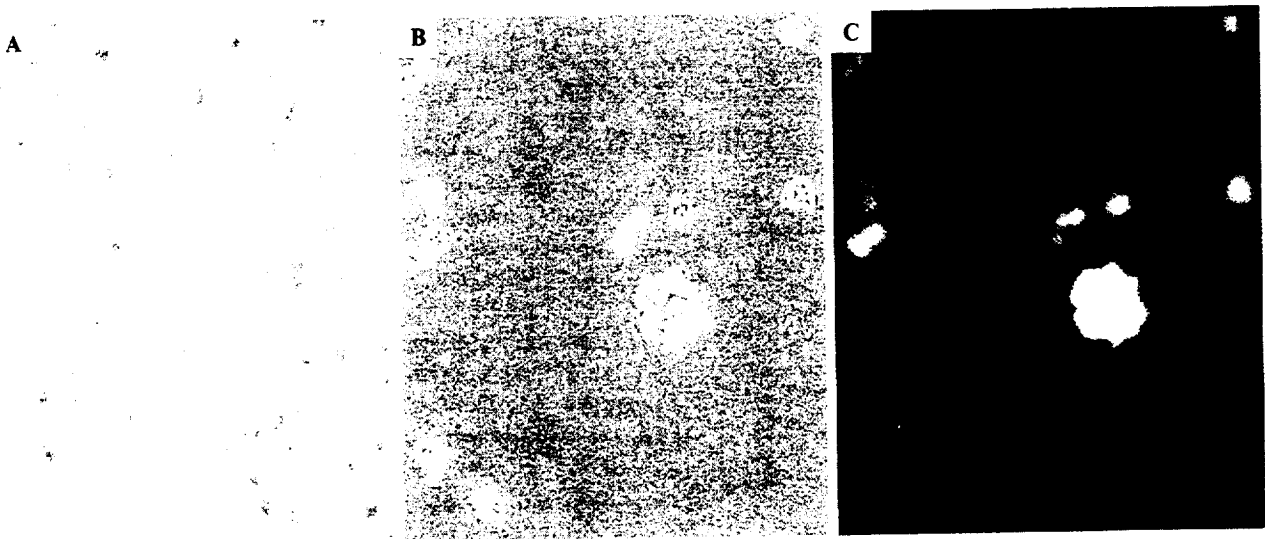


Figure 8. Morphology of hepatocytes and liver fragments after 8–10 days culture *in vitro* in a Bioreactor. Murine liver was harvested and cultured in a Bioreactor as described in Materials and methods. The morphology of the fragments including the sinusoidal structures was maintained intact for at least 8 days (A, H&E, 40 \times). Hepatocytes and smaller fragments were harvested from the Bioreactor and incubated with calcein AM to assess metabolic activity. Phase contrast (B) and fluorescence (C) demonstrate that hepatic cells still metabolize calcein AM after 10 days of cultivation in the Bioreactor.

murine breast carcinoma cells implant in the same area within the terminal portal venules or proximal hepatic sinusoids, extravasate through the periportal endothelium and then migrate to reach a subcapsular position where they proliferate to form hepatic colonies. These investigators used syngeneic tumors that may respond to appropriate microenvironmental cues. In contrast, our studies used human CRC that may not be able to respond to migratory signals from a xenogenic environment. Further, the type of migration noted by Morris *et al.* [18] was not observed by others [8] who studied experimental metastases with the murine B16F10 metastatic melanoma line. Since the B16F10 cells were initially selected for their capacity to produce lung metastases, they may not migrate through the hepatic parenchyma because they lack the ability to respond to the right migratory stimuli. However, the observation periods of these earlier studies may not have been long enough to allow the cells to migrate through hepatic parenchyma. Clearly, Barbera-Guillem *et al.* [25] observed that melanoma cells may extravasate and migrate within the space of Disse toward the central vein after entering the hepatic sinusoid. Whether other human CRC lines are capable of this migration either along the sinusoid or through the parenchyma is unknown.

A small fraction of CRC cells was detected in the lung at 4 h, after they passed through portal

venous–central venous shunts that opened at 4 h in the liver. Possibly, tumor cells may have occluded enough of the hepatic microcirculation to increase portal pressure sufficiently to open these shunts because they were observed at a time when CRC cells still remained in the portal venules. Such portal–central venous shunts may contribute to the systemic dissemination of CRC cells through the liver. Even though the data of Barbera-Guillem, Weiss and their colleagues [6–8,25] suggest that the liver entraps all cells entering through the portal vein, our own data suggest otherwise because MIP-101 colon cancer cells produce lung metastases when injected intrasplenically [23].

Since CRC cells were deformed within the terminal portal venules, we suspected that mechanical stress may be a major cause of the early death of the cells in the liver. We did not notice clasmotosis in our studies as has been reported by others [26]. Barbera-Guillem and Weiss [8] demonstrated that rapid deformation-induced trauma within the portal venous (zone 1) side of the hepatic sinusoid destroyed most of the B16 melanoma cells reaching the liver. Both Barbera-Guillem and Weiss [8] and Weiss *et al.* [27] have shown that the mechanical stress of passing through 8 μm pores in a polycarbonate membrane reproduces the type of deformation that causes the lysis of most neoplastic cells implanting in the hepatic microcirculation. To test if the human CRC cells used here were also

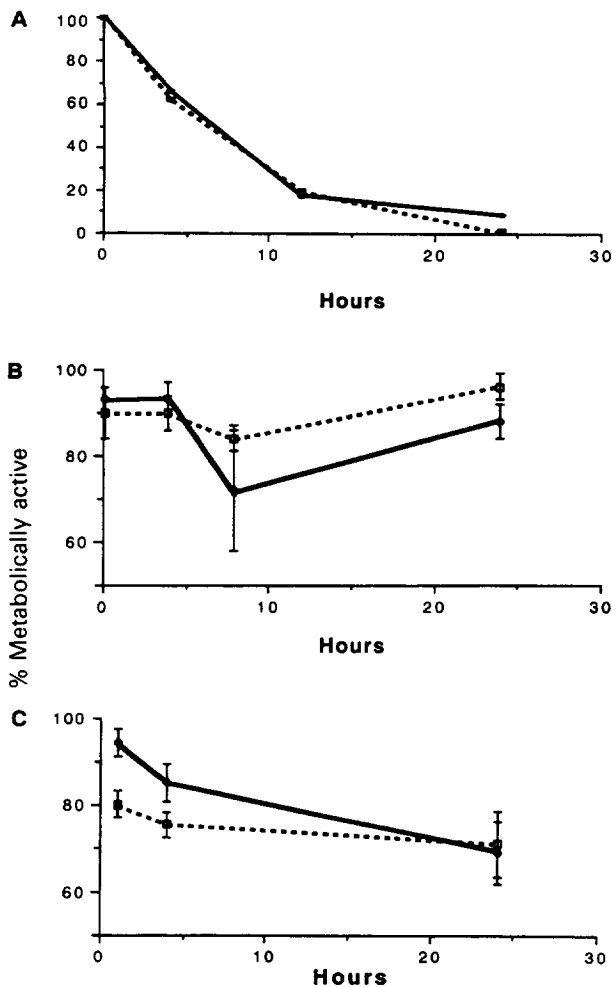


Figure 9. Percentage of CRC cells that remain metabolically active under different conditions. Double-labeled (\square) Clone A or (\bullet) CX-1 cells were either injected intrasplenically in nude mice and the livers visualized by IVFM (A), co-incubated with murine hepatic cells *in vitro* (B), or incubated in tissue culture alone (C). The percentage of metabolically active cells decreased significantly after hepatic implantation but not in the CRC-hepatic cell co-cultures or CRC cells alone *in vitro*.

% Metabolically active

$$= \frac{\text{No. of CRC cells} + \text{calcein AM}}{\text{No. of CRC cells} + \text{Rd-Dx}} \times 100.$$

susceptible to this type of mechanical stress, we passed the cells through a membrane with 8 μm pores with a constant flow at a pressure of 15 cm H_2O which is within the range of normal portal pressure [28]. Approximately 50% of both CX-1 and Clone A cells were immediately lysed during the filtration while the remaining cells passed through the membrane and remained viable even after culture for another 24 h

(data not shown). Our rate of lysis is similar to that observed by other investigators [8,27] and suggests that mechanical stress may kill a large proportion of CRC cells in the hepatic microcirculation. However, while susceptibility to mechanical stress eliminates many CRC cells, it does not ultimately determine their metastatic potential because there was no difference between the lysis of CX-1 and Clone A cells by the *in vitro* mechanical stress assay.

If susceptibility to mechanical deformation trauma does not distinguish highly from weakly metastatic cells, then another mechanism must be preventing the successful implantation of carcinoma cells. As Morris *et al.* [18] have noted, proliferation was not apparent in CX-1 cells until nearly 72 h after entrance into the liver and did not occur in any Clone A cells. However, approximately 5–10% of the Clone A cells recovered from the liver at 4 h were capable of sustained proliferation when cultured *in vitro*. These results suggest that the toxicity of the hepatic microenvironment is reversible at least at this early stage. Alternatively, Clone A cells may be more susceptible to destruction by such cytotoxic host cells as Kupffer cells or pit (natural killer or NK) cells. Some evidence of this increased sensitivity is provided by Bagli *et al.* [29], who showed that NK cells from human peripheral blood were more cytotoxic to Clone A cells than CX-1 cells. Cohen and Goldrosen [30] have also shown that the hepatic microenvironment may be especially hostile to tumor cells that implant in the liver. Thus, the critical determinant that distinguishes CX-1 and Clone A cells is that the CX-1 cells are capable of either adapting to the hepatic microenvironment and resuming proliferation or escaping the toxicity of host cytotoxic cells. However, our co-cultivation studies suggest that there is no difference in the ability of CX-1 and Clone A cells to co-exist with murine hepatocytes *in vitro* for 24 h. Possibly, the difference in survival is due to the interaction between mechanical implantation and the intimate relationship with the hepatic parenchyma which follows periportal implantation. Clearly, these experiments support the findings of earlier investigators [9–11] who advocate the seed-soil hypothesis of Paget [31] and suggest that the metastatic precursor cell must resume proliferation by adapting to its new environment within the first 24–48 h. CRC may be able to upregulate receptors for a large number of hepatic-specific factors. A number of adhesion and growth factor receptors may be activated or upregulated during such interactions and work remains to determine which factors prevent Clone A cells from proliferating.

In conclusion, the earliest phase of experimental metastasis by human CRC cells was observed in real

time by IVFM. CRC cells entering the liver by the portal vein implanted within the portal venules or proximal hepatic sinusoids in contact primarily with endothelial cells and to a lesser extent with Kupffer cells. The majority of both highly and poorly metastatic CRC cells died in the liver within 24 h while only a small proportion persisted and began to proliferate. While mechanical deformation trauma may lyse the majority of tumor cells entering the liver, the greater impediment to metastasis appears to be an inability by weakly metastatic cells to resume proliferation, possibly either because they can not use factors present in the hepatic microenvironment or because the microenvironment combined with mechanical implantation inhibits cell proliferation.

Acknowledgement

Supported by grants CA42587 and CA44704 (JM) and CA44583 (PT) from the National Institutes of Health.

References

1. Steele G Jr, Bleday R, Mayer RJ, *et al.* 1991, A prospective evaluation of hepatic resection for colorectal carcinoma metastases to the liver: Gastrointestinal Tumor Study Group Protocol 6584. *J Clin Oncol*, **9**, 1105–12.
2. Cady B and McDermott WV, 1985, Major hepatic resection for metachronous metastases from colon cancer. *Ann Surg*, **201**, 204–9.
3. Jessup JM, Giavazzi R, Campbell D, *et al.* 1989, Metastatic potential of human colorectal carcinomas implanted into nude mice: prediction of clinical outcome in patients operated upon for cure. *Cancer Res*, **49**, 6906–10.
4. Morikawa K, Walker SM, Jessup JM and Fidler IJ, 1988, *In vivo* selection of highly metastatic cells from surgical specimens of different primary human colon carcinomas implanted into nude mice. *Cancer Res*, **48**, 1943–8.
5. Jessup JM, Toth CA, Ford R, *et al.* 1993, Carcinoembryonic antigen: enhancement of liver colonisation through retention of human colorectal carcinoma cells. *Br J Cancer*, **64**, 464–70.
6. Weiss L, Nannmark U, Johansson BR and Bagge U, 1992, Lethal deformation of cancer cells in the microcirculation: a potential rate regulation of hematogenous metastasis. *Int J Cancer*, **50**, 103–7.
7. Barbera-Guillem E, Smith I and Weiss L, 1992, Cancer-cell traffic in the liver. I. Growth kinetics of cancer cells after portal-vein delivery. *Int J Cancer*, **52**, 974–7.
8. Barbera-Guillem E and Weiss L, 1993, Cancer-cell traffic in the liver. III. Lethal deformation of B16 melanoma cells in liver sinusoids. *Int J Cancer*, **54**, 880–4.
9. Liotta LA, 1986, Tumor invasion and metastasis—role of the extracellular matrix: Rhoads Memorial Award Lecture. *Cancer Res*, **46**, 1–7.
10. Nicolson GL, 1988, Organ specificity of tumor metastasis: role of preferential adhesion, invasion and growth of malignant cells at specific secondary sites. *Cancer Met Rev*, **7**, 143–88.
11. Fidler IJ, 1990, Critical factors in the biology of human cancer metastasis: Twenty-eighth G.H.A. Clowes Memorial Award Lecture. *Cancer Res*, **50**, 6130–8.
12. Burkart V and Friedrich EA, 1982, Intravital microscopy of the perfused liver: sinusoidal cells trap xenogeneic erythrocytes and tumor cells. *J Reticuloendothelial Soc*, **32**, 269–72.
13. Arndt-Jovin A and Jovin TM, 1989, Fluorescence labeling and microscopy of DNA. In: Wang Y-L and Tayler DL, eds. *Fluorescence Microscopy of Living Cells in Culture, Part B*. Academic Press, Inc., San Diego, CA, pp. 417–48.
14. Moore PL, MacCoubrey IC and Haugland RP, 1990, A rapid, pH insensitive, two color fluorescence viability (cytotoxicity) assay. *J Cell Biol*, **111**, 58a.
15. Weiss L, 1993, Deformation-driven destruction of cancer cells in the microvasculature. *Clin Exp Metastasis*, **11**, 430–3.
16. Chambers AF, Schmidt EE, MacDonald IC, Morris VL and Groom AC, 1992, Early steps in hematogenous metastasis of B16F1 melanoma cells in chick embryos studied by high-resolution intravital videomicroscopy. *J Natl Cancer Inst*, **84**, 797–803.
17. McDonald IC, Schmidt EE, Morris VL, Chambers AF and Groom AC, 1992, Intravital videomicroscopy of the chorioallantoic microcirculation: a model system for studying metastasis. *Microvascular Res*, **44**, 185–99.
18. Morris VL, Koop S, MacDonald IC, *et al.* 1994, Mammary carcinoma cell lines of high and low metastatic potential differ not in extravasation but in subsequent migration and growth. *Clin Exp Metastasis*, **12**, 357–67.
19. McNeil PL, Murphy RF, Lanni F and Taylor DL, 1984, A method for incorporating macromolecules into adherent cells. *J Cell Biol*, **98**, 1556–64.
20. McNeil PL, 1989, Incorporation of macromolecules into living cells. In: Wang Y-L and Tayler DL, eds. *Fluorescence Microscopy of Living Cells in Culture, Part A*. Academic Press, Inc., San Diego, CA, pp. 153–73.
21. Post S, Menger MD, Rentsch M, *et al.* 1992, The impact of arterialization on hepatic microcirculation and leukocyte accumulation after liver transplantation in the rat. *Transplantation*, **54**, 789–94.
22. Kawano K, Bowers JL, Kruskal JB and Clouse ME, 1995, *In vivo* microscopic assessment of hepatic microcirculation during liver allograft rejection in the rat. *J Hepatol*.
23. Wagner HE, Thomas P, Wolf BC, *et al.* 1990, Characterization of the tumorigenic and metastatic potential of a poorly differentiated human colon cancer cell line. *Invasion Metastasis*, **10**, 253–66.
24. Jessup JM, Goodwin TJ and Spaulding G, 1993, Prospects for use of microgravity-based bioreactors to study three-dimensional host-tumor interactions in human neoplasia. *J Cell Biochem*, **51**, 290–300.
25. Barbera-Guillem E, Smith I and Weiss L, 1993, Cancer-cell traffic in the liver. II. Arrest, transit and death of B16F10 and M5076 cells in the sinusoids. *Int J Cancer*, **53**, 298–301.

S. Ishii et al.

26. Morris VL, MacDonald IC, Koop S, et al. 1993, Early interactions of cancer cells with the microvasculature in mouse liver and muscle during hematogenous metastasis: videomicroscopic studies. *Clin Exp Metastasis*, **11**, 377-90.
27. Weiss L, Elkin G and Barbera-Guillem E. 1993, The differential resistance of B16 wild-type and F10 cells to mechanical trauma *in vitro*. *Inv Metast*, **13**, 92-101.
28. McCuskey RS and Reilly FD, 1993, Hepatic microvasculature: dynamic structure and its regulation. *Sem Liver Dis*, **13**, 1-12.
29. Bagli DJ, Steele GD Jr and Barlozzari T, 1989, Natural killer sensitivity of colorectal carcinoma targets. Correlation with degree of differentiation. *Arch Surg*, **124**, 89-93.
30. Cohen SA and Goldrosen MH, 1989, Modulation of colon-derived experimental hepatic metastasis by murine nonparenchymal liver cells. *Immunol Invest*, **18**, 351-63.
31. Paget S, 1889, The distribution of secondary growths in cancer of the breast. *Lancet*, i, 571-3.

Appendix 3

J.M. Jessup

**Role of Nitric Oxide and Superoxide Anion in Hepatic Endothelial Cell Toxicity
to Human Colorectal Carcinomas**

Kirsten H. Edmiston, Yutaka Shoji, Takayuki Mizoi, Rosilyn Ford,
Alexander Nachman, and J. Milburn Jessup

Laboratory of Cancer Biology, Department of Surgery, Beth Israel Deaconess Medical Center,
Harvard Medical School, Boston Massachusetts 02115, USA.

Running title: SINUSOIDAL ENDOTHELIAL CELLS KILL TUMOR CELLS

Correspondence and address requests for reprints to: J.M. Jessup, M.D., Department of Surgery,
Beth Israel Deaconess Medical Center, 110 Francis Street Suite 3-A, Boston, MA 02215.

Telephone: (617) 632-9817; Facsimile: (617) 632-7424; Electronic mail: jessupj@delphi.com

This work was supported by grants to JMJ from the National Cancer Institute (CA 42857 and CA
44704) and from the National Aeronautics and Space Administration (NAG 9-650) as well as
Surgical Oncology Training Grant T32-CA 9850 to KHE.

Abbreviations: CRC: colorectal carcinoma; DEX: dexamethasone; LDL: low density lipoprotein; GaCl_3 : gadolinium chloride; cNOS: constitutive nitric oxide synthase; iNOS: inducible nitric oxide synthase; NMMA: N^G -monomethyl-L-arginine; NO: nitric oxide; O_2^- : superoxide anion; PEG-CAT: polyethylene glycol-catalase; PEG-SOD: polyethylene glycol-superoxide dismutase; Rd-Dx: rhodamine B isothiocyanate-dextran; SEC: sinusoidal endothelial cells; SIN-1: 3-morpholinosydnonimine N-ethylcarbamide; SNP: sodium nitroprusside; SOD: superoxide dismutase.

Key words: endothelial cell, tumor cell lysis, liver metastasis, nitric oxide, reactive oxygen species, colorectal carcinoma.

ABSTRACT

Human colorectal carcinoma (CRC) cell survival for the first 24 hour after implantation in the hepatic sinusoid determines its potential to colonize the liver. Nearly ten-fold more highly metastatic CX-1 cells survive within the livers of nude mice 24 hours after intrasplenic injection than weakly metastatic Clone A cells. Since CRC contact sinusoidal endothelial cells (SEC) during implantation, we sought to determine whether SEC were more toxic to Clone A than CX-1 cells. When 2×10^4 vital dye-labeled CRC were added to murine SEC monolayers, more than 30% of Clone A cells lost calcein AM fluorescence compared to less than 5% of CX-1 cells after 24 hr of coculture with SEC. Kupffer cells did not mediate this effect because neither enriched Kupffer cells nor SEC treated with a Kupffer cell inhibitor altered the SEC-mediated toxic effect to Clone A cells. Pretreatment with a nitric oxide synthase inhibitor N^G -monomethyl-L-arginine (NMMA), superoxide dismutase (SOD), or dexamethasone blocked SEC-mediated toxicity to Clone A cells, whereas calcium chelation and catalase did not. In addition, Clone A cells were more sensitive to a superoxide donor, 3-morpholinosydnonimine N-ethylcarbamide, than CX-1 cells and neither cell line was sensitive to sodium nitroprusside, a nitric oxide donor. Thus, unstimulated murine SEC produce reactive oxygen species that are selectively toxic to weakly metastatic Clone A cells. This may be a mechanism by which host liver cells remove weakly metastatic neoplastic cells.

INTRODUCTION

Metastasis occurs when circulating tumor cells implant in a microcapillary bed, penetrate the endothelium, and proliferate within the parenchyma (1, 2). Since the first step involves intimate tumor-endothelial cell contact (3, 4), the SEC may have an important role in determining the ability of metastatic precursor cells to implant and proliferate. Cytokine-activated murine pulmonary endothelial cells lyse murine tumor cells (5) which is partially mediated by nitric oxide (NO) produced by cytokine-activated endothelial cells (6). However, endothelial cells are not usually activated by cytokines prior to tumor cell implantation. Since human colorectal carcinoma (CRC) cells primarily contact SEC during implantation in athymic nude mouse liver (7), we postulated that SEC unstimulated by exogenous cytokines may inhibit the growth of a human CRC line that has weak potential to colonize the liver.

Our purpose in these studies was to assess the ability of unstimulated murine SEC to be cytotoxic and/or cytostatic to weakly or highly metastatic human CRC. Highly metastatic human CRC cells produce liver colonies in 50 - 100% of athymic nude mice within 60 days after the intrasplenic injection of 2×10^6 viable tumor cells while weakly metastatic CRC cells only produce liver colonies in 20% or fewer mice after the same dose of tumor cells (8, 9). The ability of human CRC to colonize the livers of nude mice is associated with the ability of these CRC to recur and metastasize in the original patient (10). As a result, the intrasplenic model may provide a means of assessing some of the mechanisms involved in metastasis to the liver, which is the most common visceral site of metastasis in patients. Ishii et al (7) demonstrated that highly and weakly metastatic CRC cells behaved differently during the first 24 hour after their arrest in the liver. Viable CX-1 and Clone A CRC (2×10^6 cells/ mouse) were injected intrasplenically and their passage into the hepatic sinusoids followed by intravital fluorescence microscopy (7). Nearly ten-fold more CX-1 cells were alive 24 hr after implantation than Clone A cells (6 ± 2 for CX-1 cells/ mm^2 compared to 0.7 ± 1 Clone A cells/ mm^2) (7). CX-1 cells formed 4 - 8 cell colonies at 72 hr when only a few, single Clone A cells were detectable (7). Ultimately, CX-1 forms liver colonies in more than 90%

of mice injected intrasplenically with 2×10^6 viable cells compared to only 2% of mice injected with Clone A cells (8). Since both CRC lines arrest in close contact with SEC, SEC may be more toxic to Clone A than CX-1 cells.

Our present approach to test this postulate was to establish short term monolayer cultures of murine SEC that were then overlaid with CX-1 and Clone A cells. The results suggest that more weakly metastatic Clone A cells are killed by SEC than CX-1 cells. Furthermore, inhibitors of nitric oxide synthase or superoxide anion block this effect. Thus, SEC have an active role in preventing the establishment of liver metastasis by some colorectal carcinoma cells.

MATERIALS AND METHODS

Animals

Six- to 8-week old male Swiss mice weighing 30-40 g were obtained from Harlan Sprague-Dawley Inc. (Indianapolis, IN) and kept under specific pathogen-free condition. The standard diet and water were given *ad libitum*. SEC isolation was performed under general anesthesia with intraperitoneal administration of sodium pentobarbital (50 mg/Kg, Abbott Laboratories, North Chicago, IL). All animal experiments were approved by the Animal Care and Use Committee of the Beth Israel Deaconess Medical Center and were conducted in accordance with the guidelines issued by the National Institutes of Health for the care of laboratory animals.

Human colorectal carcinoma cell lines

Clone A, a poorly differentiated human CRC, was obtained from D.L. Dexter, Dupont Demours & Co., Wilmington, DE and is weakly metastatic since it produces liver colonies in 2% of mice injected with 2×10^6 cells intrasplenically (8). CX-1, a moderately differentiated human CRC line, is a highly metastatic CRC line because it produces liver colonies in 93% of mice after intrasplenic injection (8) and was provided by Dr. L.B. Chen (Dana-Farber Cancer Institute, Boston, MA). The CRC lines were maintained in RPMI 1640 medium with 10% fetal bovine

serum (FBS; SIGMA Chemical Company, St. Louis, MO), 1 % L-glutamine (GIBCO), 100 units/ml of penicillin G (GIBCO) and 100 mg/ml of streptomycin (GIBCO) (1 % P/S). Both CRC lines were checked for the presence of mycoplasma by GEN-PROBE, mycoplasma T.C., rapid detection system (GEN-PROBE Inc., San Diego, CA) and were negative.

Isolation of murine hepatic endothelial cells

The procedure for the isolation of hepatic endothelial cells is a modification of a method that uses collagenase infusion followed by metrizamide density gradient and selective adherence (11, 12). Briefly, the liver cells were dispersed by perfusion through the portal vein with Ca^{++} and Mg^{++} free buffer containing 0.83% sodium chloride, 0.05% potassium chloride and 0.005 M M-(2-hydroxylmethyl) piperazine-N (2-ethanesulfonic acid), (HEPES), followed by the perfusion of 0.05 % collagenase (0.025 % type II and 0.025 % type IV) and 0.0003 % DNase in GBSS. Perfusion was performed at a flow rate of 5 ml/min for 2 min. The liver was then removed, incubated for 15 min at 37°C in 5% CO_2 , minced after removing the gallbladder and Glisson's capsule and then passed through a 150 μm steel grid. The cell suspension was centrifuged in GBSS at 50 x g for 2 min at 4 °C. The pellet containing hepatocytes was discarded, and the supernatant was centrifuged again at 300 x g for 10 min at 4°C. The murine SEC were separated from this cell pellet by isopycnic sedimentation using a metrizamide gradient in which pelleted cells resuspended in 5 mL of GBSS were mixed with an equal volume of a 30% metrizamide solution in GBSS without NaCl and 1 ml of GBSS was then gently layered on top of the metrizamide-cell mixture. This gradient was then centrifuged 860 x g at the interface layer at 20°C for 20 min (Beckman L8-M, ultracentrifuge SW-41Ti swing rotor). SEC were aspirated from the interface and incubated in MCDB 131 medium for 30 min at 37°C on Petri dishes. Since Kupffer cells attach and spread quickly on plastic surfaces (13), the plates were aspirated and washed once with the nonadherent cells collected to remove Kupffer cells. The cells were resuspended in MCDB 131 medium with 5 % FBS, 1 $\mu\text{g}/\text{ml}$ hydrocortisone, 1 % L-glutamine and 1 % P/S and the number of cells and viability determined. SEC were seeded on fibronectin coated 96 well microtiter plates

(Costar, Cambridge, MA) at 2×10^5 cells/well. The non-attached cells were removed by washing five times 2 hrs after seeding and the culture medium was changed every 24 hrs. The purity of SEC was evaluated by their uptake of acetylated human low density lipoprotein labeled with the fluorescent probe 1,1'-dioctadecyl-1-3,3',3'-tetramethyl-indocarbocyanine perchlorate (DiI-Ac-LDL) (Biomedical Technologies, Inc.) (14). Cells were incubated for 4 hr in $10\mu\text{g/ml}$ DiI-Ac-LDL in MCDB 131 media, then washed in PBS, as described in the instructions provided by the manufacturer.

Isolation of murine Kupffer cells

For the isolation of Kupffer cells, the method of Phillips et al. (15) was modified. Briefly, the initial perfusion and digestion were performed as described above for isolation of SEC. However, the cell pellet was resuspended in 2.5 ml of GBSS and mixed with 3.5 ml of 30% metrizamide in GBSS without NaCl, overlaid with 1.0 ml GBSS with NaCl and centrifuged at $1264 \times g$ at the interface for 20 min at 20°C (15). Cells were aspirated from the interface and incubated for 20 min at 37°C in T 25 culture flasks. The attached Kupffer cells were cultured in RPMI 1640 media with 10% FBS, 1% glutamine, and 1% P/S at 37°C in 5% CO_2 . Kupffer cells were identified by phagocytosis of $3.015 \mu\text{m}$ Latex-beads (16).

Metabolic Activity and Cell Proliferation Assays

To evaluate the metabolic activity of CRC cells by fluorescence microscopy, CRC cells were labeled with two fluorescing reagents, rhodamine B isothiocyanate-dextran (Rd-Dx) with a maximum excitation/emission at 530/590 nm and calcein AM with a maximum excitation/emission at 485/530 nm. Rd-Dx was loaded into CRC cells by electroporation (The ElectroPorator, Invitrogen Corporation, San Diego, CA). CRC cells were suspended in 20 mg/ml Rd-Dx in RPMI 1640 and received 300 volts, 50 watts and 50 mA (Capacitance: $1000\mu\text{F}$, 330 Vmax, Load resistance: $\infty\Omega$). The Rd-Dx loaded cells were incubated for 24 hr at 37°C in complete tissue culture medium and then adherent cells were recovered by trypsin. The cells were suspended in

PBS and incubated with 4 μ M calcein AM for 1 hr at 37°C. Calcein AM was used to detect viable cells because it only produces strong fluorescence in live cells with ATP-dependent cytoplasmic esterase activity (17). After washing with PBS, the cells were suspended in MCDB 131 medium and 2×10^4 cells seeded on SEC monolayers. At least 90% of the cells were labeled with both fluorescent markers in each experiment. The SEC monolayers were analyzed by fluorescence microscopy at up to 24 hr after addition of CRC. The % metabolic activity was calculated to be equal to the number of calcein positive and Rd-Dx positive cells divided by the total number of Rd-Dx positive cells expressed as a percentage. Each assay was performed in quadruplicate.

Cell proliferation was measured using a crystal violet assay. Cells were seeded in 96 well microtiter plates. At the indicated time, each well was washed once with PBS. Then 100 μ l of a 1% glutaraldehyde solution was added to each well for 10 min at 23°C when 100 μ l of 0.2% Triton X-100 was added. Fifty ml of 0.1% crystal violet was added to each well at 37°C for 30 min. Plates were read at 600 nm for absorbance on a 96 well microtiter plate reader (model 2550 EIA reader, Bio-Rad Lab., Richmond CA).

Inhibition of SEC Toxicity

SEC were treated with Gadolinium chloride (GaCl_3) according to the method of Saad *et al.*, (18) to inhibit Kupffer cell function. SEC were incubated with 10 μ g/ml GaCl_3 in medium 24 hrs after plating. After 12 hrs at 37°C, the plates were washed and fresh medium added. Clone A or CX-1 (5×10^4 cells/well) cells labeled with Rd-Dx and calcein AM were added and cocultured with SEC monolayers. In some experiments, CRC were exposed to GaCl_3 for up to 96 hr and then % Metabolic Activity and proliferation were determined in the absence of SEC.

SEC monolayers were also incubated with 1 to 10^{-6} mM of N^G -monomethyl-L-arginine (NMMA), a specific inhibitor of nitric oxide synthesis, when CRC were added to determine the role of nitric oxide (NO). In other experiments SEC-CRC cocultures were also incubated with 10 mM EDTA or 10 μ g/ml dexamethasone (both from Sigma Chemical Co., St. Louis, MO). After 24 hr coculture, the % metabolic activity of the CRC and nitrite were measured.

In some experiments the role of superoxide anion and peroxides was also analyzed. Superoxide Dismutase (SOD) or catalase (CAT) (Oxis International, Inc., Portland, OR) was added at final concentrations of 0.001 to 1 mM with the tumor cells to SEC monolayers. Co-cultures were then incubated for 24 hr and then analyzed as above. CX-1 or Clone A cells alone (2×10^4 cells/200 μ l of standard complete medium in uncoated 96-well microtiter plates) were exposed alone for 48 hr to sodium nitroprusside (SNP) or 3-morpholinopyridone N-ethylcarbamide (SIN-1) at 10 to 200 μ M to determine the relative sensitivity of the CRC lines to NO or to superoxide anion. Toxicity was measured by inhibition of cell proliferation in the crystal violet assay described above.

NO, SOD and Cytokine Assays

To assess the production of NO by SEC and CRC, the concentration of nitrite was measured using the Griess reaction as described previously (19). After 24 hrs of coculture, 50 μ l of culture medium was incubated at 23°C with 50 μ l of a 1:1 mixture of 2% sulfanilamide in 5% phosphoric acid with 0.2% N-(1-naphthyl)ethylenediamine dihydrochloride in water. After 10 min, absorbance at 550 nm was measured using a microplate reader (model 3550 EIA reader, Bio-Rad Lab., Richmond CA). Nitrite concentrations were determined by comparison with a standard solution of sodium nitrite (NaNO_2) in water. SOD activity was measured in CRC cells by the method of Oyanagi (20). In some experiments the amount of murine IL-6, IL-1 α and TNF- α were determined by enzyme immunoassay using commercially available kits (Endogen, Inc., Woburn, MA).

Statistical Analysis

The results of the CRC - SEC adhesion and the % metabolic activity assays are expressed as mean \pm SEM with differences among groups of means tested by one-way analysis of variance (ANOVA). All assays were performed in quadruplicate and repeated at least once. When ANOVA demonstrated that means within an experiment were significantly different from one another,

significance between individual group means was tested with the Fisher PSLD with a significance level of 5%. All calculations were performed on a Macintosh Quadra 950 microcomputer using Statview SE+Graphics (Abacus Concepts, Inc., Berkeley, CA).

RESULTS

Isolation and culture of murine hepatic SEC

An average of $5.2 \pm 0.6 \times 10^6$ SEC/gm of liver were isolated from young adult male Swiss mice using the collagenase perfusion method. SEC attached to a fibronectin-coated substrate during the first two hours in MCDB 131 medium and formed monolayers within 48 hr (Fig. 1 A). After 48 hr, 92 ± 3 % of SEC were DiI-Ac-LDL positive endothelial cells (Fig. 1B), and 97 ± 3 % were calcein AM positive (Fig. 1 C). Only 8 ± 1 % of cells phagocytosed $3.0 \mu\text{m}$ latex beads and appeared to be Kupffer cells. Thus, the monolayers contained more than 90% endothelial cells and were more than 95% viable.

Morphological changes in CRC cells during SEC coculture

The morphology of SEC-CRC cocultures were studied by light microscopy to determine whether SEC affected the ability of Clone A cells to spread and proliferate during coculture. 2×10^4 CRC cells / well were cocultured with SEC at a SEC-CRC ratio estimated to be 10 : 1 for up to 72 hr. CRC cells were also cultured on standard tissue culture plastic surfaces as controls. At 24 hr of coculture, CX-1 cells were aggregated (Fig. 2D), while Clone A cells that were still intact were single, round and isolated (Fig. 2C). Clone A cells formed small 2 - 4 cell aggregates by 48 hr (Fig. 2E), whereas CX-1 cells had spread to form colonies that were almost confluent within the microtiter wells (Fig. 2F). Since both Clone A and CX-1 cells readily attach and spread on plastic (Fig. 2G and 2H), SEC appear to inhibit both the spreading and colony formation by Clone A cells but not CX-1 cells for the first 24 hr of coculture.

Effect of cocultures on the % metabolic activity of CRC cells

We next investigated whether SEC affected the viability and proliferative capacity of CRC. CRC prelabeled with Rd-Dx and calcein AM were added to SEC monolayers in 96-well plates at SEC to CRC ratios of 10:1 and fluorescence assessed at intervals up to 24 hr. The metabolic activity of both Clone A and CX-1 decreased over time (Fig. 3). However, the percentage of Calcein AM positive Clone A cells was significantly lower than that of CX-1 between 4 and 24 hr with 32% of Clone A cells losing calcein AM fluorescence compared to only 5% of CX-1 cells after 24 hr of coculture with SEC (Fig. 3). These data suggested that SEC monolayers were more toxic to the weakly metastatic Clone A cells compared to the highly metastatic CX-1 cells.

The loss of calcein AM fluorescence is an indirect measure of cell toxicity (15). Another measure of cellular toxicity involves inhibition of proliferation. To determine whether SEC also inhibited the proliferation of Clone A cells, Clone A and CX-1 cells were recovered after different times of coculture with SEC, and recultured in fresh medium. Proliferation was assessed over a subsequent 72 hr. Both the yield of Clone A cells (Fig. 4A) and the viability of the recovered cells (Fig. 4B) decreased over the first 24 hr (by 27% and 17%, respectively) so that the proportion of viable Clone A cells available for reculture decreased to 59% by 24 hr (Fig 4C). However, Clone A cells cultured with SEC for only 1 or 4 hr showed the same pattern of proliferation as freshly isolated Clone A cells (Fig. 5). In contrast, Clone A cells recovered 8 or more hr after coculture with SEC did not begin to proliferate within 72 hr of reculture (Fig. 5). Thus, SEC exert a cytotoxic and cytostatic effect that causes a profound inhibition of cell proliferation that persists in Clone A cells that have been cultured with SEC for 8 or more hrs.

Endothelial cells mediate SEC toxicity

Since SEC are enriched for endothelial cells but contain 5% - 10% Kupffer cells, it is possible that the toxic effect of SEC is mediated by Kupffer cells rather than by endothelial cells. Several experiments suggest that the endothelial cells are the active inhibitory population rather than the Kupffer cells. First, enriched murine Kupffer cell preparations at ratios of 10 Kupffer cells: 1

CRC cell induced less than 5% loss of calcein AM fluorescence in either Clone A or CX-1 cells after 24 hr of coculture (data not shown). Second, incubation of SEC with 10 $\mu\text{g/ml}$ gadolinium chloride (GaCl_3) inhibited Kupffer cell phagocytic function by 59% (data not shown), but did not block SEC-mediated toxicity to Clone A cells: Clone A cells in SEC co-culture with GaCl_3 displayed a $75 \pm 4\%$ Metabolic Activity compared to $68 \pm 3\%$ for Clone A cells cultured for 24 hr with SEC but without GaCl_3 , $P=\text{NS}$. Since GaCl_3 pretreatment at doses that inhibit phagocytosis also block the ability of Kupffer cells to kill tumor cells (21), the experiments with GaCl_3 suggest that SEC rather than Kupffer cells are toxic to Clone A cells.

Cytokine Production By SEC Cocultured With Human CRC

Exogenous cytokines activate endothelial cells to be cytotoxic to tumor cells (5) but SEC may produce cytokines on co-culture with CRC that then mediate the loss of Clone A cells. The spent media from the cultures of SEC alone, CRC alone, and the SEC-CRC cocultures were examined for their content of the murine cytokines IL-1 α and TNF- α after 24 hr of coculture. Media from human CRC cells cultured alone did not contain murine cytokines (data not shown). The murine SEC cultured alone produced approximately 29 pg/mL of IL-1 α and no detectable TNF- α . SEC cultured with either CX-1 or Clone A cells did not produce more IL-1 α or TNF- α (data not shown). These results suggest that the toxic effect of SEC on CRC is not likely to be mediated by the inflammatory cytokines IL-1 α or TNF- α .

The Role of Nitric Oxide in Clone A Cell Toxicity

Nitric oxide (NO) is an important regulatory molecule produced by both endothelial and Kupffer cells. When CRC cells were cocultured with confluent SEC monolayers for 24 hr, NO production was measured indirectly by assaying the amount of nitrite formed in the conditioned medium. Cultures of SEC and Clone A by themselves did not produce detectable amounts of NO whereas CX-1 produced 9.4 μM nitrite (Table 1). However, when the human CRC cell lines were cultured with SEC, the conditioned media only contained 2.2 - 8.5 μM nitrite (Table 1).

To further examine the role of NO in the interaction between SEC and Clone A cells, Clone A cells were cocultured with SEC in the presence of NMMA, a specific nitric oxide synthase inhibitor. NO production and the toxic effect of SEC were inhibited significantly by doses of NMMA greater than 10^{-4} mM (Fig. 6). Doses greater than 1 mM of NMMA did not effect the viability or proliferation of Clone A cells (data not shown). When Clone A and CX-1 cells were exposed for 48 hr to 0.019 - 1.9 mM of sodium nitroprusside, a NO donor, at concentrations that are at least two orders of magnitude greater than that measured in the media of SEC cocultures, they remained viable and proliferated as well as untreated controls (Fig. 7A). When other inhibitors were assessed for their effect on SEC-mediated toxicity to CRC, dexamethasone but not EDTA inhibited SEC toxicity to Clone A (Table 2). NO is toxic to tumor cells but requires concentrations that are at least an order of magnitude greater to kill tumor cells than are detectable in our cultures (5). These results suggest that Clone A cells are not intrinsically more sensitive to exogenous NO than CX-1 cells and also support a regulatory rather than direct toxicity role for NO.

SEC also produce superoxide (O_2^-) and peroxides that may be toxic to CRC. To test the toxicity of these reactive oxygen species, Clone A and CX-1 cells were added to SEC monolayers in the presence of SOD or CAT that scavenge O_2^- and peroxides, respectively. Neither SOD nor CAT affected the viability of CX-1 cells cultured with SEC (Table 3). However, SOD blocked nearly 60% of the SEC-mediated toxicity to Clone A cells whereas CAT did not (Table 3). When CX-1 and Clone A cells were incubated with SIN-1, an O_2^- donor, the proliferation of Clone A, but not CX-1, cells was inhibited (Fig. 7B). Finally, lysates of Clone A cells contained 15% less SOD activity than CX-1 cells: 5.26 units/mg protein vs 6.19 units/mg protein. These results suggest that Clone A cells are more sensitive to O_2^- and related compounds than CX-1 cells and support the concept that SEC-mediated toxicity involves O_2^- .

DISCUSSION

Our studies suggest that hepatic SEC use NO and O₂⁻ to inhibit the growth of weakly metastatic Clone A human colorectal carcinoma cells. We focused on the interaction between tumor cells and SEC because intravital videomicroscopy studies (7, 22) suggest that tumor cells most commonly impact against the endothelium lining the periportal hepatic sinusoids. This impaction occurs in sinusoids that are not stimulated by pretreatment with cytokines. As a result, it is important to assess the function of unstimulated cells lining the hepatic sinusoid in order to elucidate how host cells interact with tumor cells during implantation. We found that the *in vitro* effects of SEC on CRC viability parallel the ability of these two CRC cell lines to survive in mouse liver. To our knowledge, this is the first report that untreated hepatic SEC may be toxic to carcinoma cells. Certainly, Li and colleagues (5, 6) have demonstrated that mouse pulmonary microvessel endothelial cells kill metastatic tumor cells if activated by pretreatment with cytokines. Furthermore, Rocha *et al.* (23) have demonstrated that liver endothelial cells participated in T-cell-dependent host resistance to lymphoma metastasis in the liver through the release of NO. Our results extend these earlier observations because they suggest that the metastatic potential of human CRC may be related inversely to their sensitivity to SEC-mediated growth inhibition.

Monolayers of hepatic SEC were necessary to adequately test the possibility that the endothelium was toxic to the CRC. The collagenase perfusion technique modified from the procedure of Smedsrød (11) and Knook et al (24) provides an excellent cell suspension which forms monolayers readily with retention of functional activity (25 - 27). The isolated SEC were similar to those described by Smedsrød et al (11). Although Braet *et al.* (28) reported that they were not able to culture SEC for longer than 4 days, our SEC cultures maintained viability for at least 7 days which was probably due to the use of a medium that was optimized for human microvascular endothelial cell culture. Unfortunately, we found that murine hepatic sinusoidal endothelial cells only underwent 3 - 4 divisions before becoming quiescent. This prevented us from cloning these cells to isolate them to purity as Li *et al.* (5) did in their initial studies.

However, our data suggest that endothelial cells are the toxic effector cell because 1) 10:1 ratios of enriched populations of Kupffer cells to tumor cells were not toxic to CRC and 2) doses of GaCl₃ that inhibit tumoricidal or static activity by Kupffer cells (21) did not block SEC toxicity to CRC. Attempts to clone the hepatic endothelial cell will have to await the development of a better medium to support their continued proliferation.

SEC may have been partially activated during their isolation from the liver. While all materials used were endotoxin-free, non-parenchymal cell populations may be activated during isolation because endogenous pyrogens may be present or liberated into the portal blood of certain species and lead to low level chronic activation of both parenchymal and non-parenchymal cells (29). However, the low levels of nitrite and cytokines suggest that the SEC were not activated significantly during their isolation.

NO is produced by endothelial cells (30) and may have cytostatic effects on tumor cells (31, 32). NO is derived from the terminal guanido-nitrogen of L-arginine (33, 34) by two constitutive nitric oxide synthases (cNOS) or one inducible nitric oxide synthase (iNOS) (32, 35, 36). The two cNOS enzymes are present in endothelial cells and brain, whereas iNOS is produced in inflammatory cells and endothelial cells. Cells expressing a cNOS rapidly and transiently produce small amounts of NO, whereas cells expressing iNOS produce larger amounts of NO after an induction phase (37). Several recent reports suggest that normal and neoplastic colonic epithelial cells produce both cNOS and iNOS (38 - 41). The amount of NO produced in our cocultures is low (0 - 9 μ M) compared to the amount present in the cultures of Li *et al.*, (6) who observed that concentrations greater than 80 μ M of NO were associated with significant tumor lysis. The sensitivity of Clone A cells to SEC is not likely to be due to the NO produced by the SEC in these experiments since exposure of CRC to SNP at NO concentrations at least two orders of magnitude greater than was present in the CRC-SEC cocultures was not toxic to Clone A. In addition, the protein levels of cNOS and iNOS in CRC and SEC cultures were low as assessed by western blot and did not increase during the short period of co-culture (data not shown). However, NO may regulate the function of nuclear transcription factors that control cytokine and

oxygen radical production (42). Inhibition of the low levels of NO seen in these cultures may have profound effects on the expression of other cytotoxic mechanisms. The ability of dexamethasone to inhibit SEC toxicity to Clone A cells supports such a possibility. The low levels of IL-1 α and TNF- α present in the CRC-SEC cocultures also suggest that these cytokines are not the cause of death of Clone A cells. Interestingly, incubation with either murine or human recombinant IL-1 α or TNF- α was not growth inhibitory to Clone A or CX-1 even at doses that were ten-fold higher than in the CRC-SEC cocultures (data not shown). Further work is necessary to elucidate these points, but our data support a role for NO as an intermediate regulator rather than proximate effector of toxicity to tumor cells.

Superoxide anion and related species appear to be the toxic mediator of the SEC effect since SOD and not catalase blocked the effect of SEC and the O₂- donor SIN-1 was toxic to Clone A cells with kinetics that were similar to that of the SEC-mediated effect. The roles of reactive oxygen species and antioxidants within carcinomas are controversial. Reactive oxygen species include NO, O₂⁻, and peroxides and have effects on tumor cells that are similar to ionizing radiation in that they may cause DNA damage as well as lipid peroxidation and protein oxidation (43). These reactive oxygen species may either kill tumor cells or accelerate genomic instability and promote tumor progression (44). The levels of reactive oxygen species are increased in colorectal carcinoma and polyps (45, 46). Arrayed against the oxidative potential of these reactive oxygen species are the antioxidants SOD, catalase, glutathione peroxidase, and Bcl-2 among others (47). Several investigators have found in colorectal carcinoma that the levels of SOD2 activity are increased in primary colorectal carcinomas (48 - 50), although others (51, 52) observed a decrease in SOD activity. Interestingly, SOD activity has been directly associated with aneuploidy (50) which may be an indicator of an aggressive cancer. The net balance of antioxidants and reactive oxygen species may determine the ability of tumor cells to respond to oxidative stress. The lower level of SOD activity in Clone A cells may be associated with a decreased ability to survive the oxidative stress produced by SEC. Finally, since exogenous SOD decreased the SEC-mediated toxicity by slightly more than 50%, other mechanisms of cell death may account for the remaining

toxicity. Either another anti-oxidant defense mechanism such as Bcl-2 or glutathione peroxidase is decreased in Clone A cells or there may be a second mechanism of cell death present. Future work remains to sort out these possibilities.

The pattern of SOD and NMMA inhibition of SEC-mediated toxicity combined with sensitivity to SIN-1 raises the possibility that O_2^- may not be the ultimate mediator of toxicity. Squadrito and Pryor (53) have shown that NO and O_2^- combine to produce peroxynitrite which is highly reactive and may explain the low levels of nitrite observed in our data. Attempts to assess directly O_2^- and peroxide concentration in SEC with fluorescent probes demonstrated that Clone A tended to increase the relative amount of both reactive oxygen species in SEC whereas CX-1 did not (data not shown). Possibly, peroxynitrite is the active mediator.

In summary, murine SEC affected the viability and proliferation of weakly metastatic Clone A human CRC more than highly metastatic CX-1 cells. As a result, SEC may have a major effect in determining the establishment of metastasis by colorectal carcinoma. The nature of the sensitivity of the weakly metastatic CRC or the resistance to SEC toxicity by the highly metastatic CRC is of practical importance and needs to be elucidated further. Modulation of the ability of SEC to produce NO and O_2^- may have important consequences for the establishment of metastases.

REFERENCES

1. Fidler, I.J., and Balch, C.M. The biology of cancer metastasis and implications for therapy. *Curr. Probl. Surg.* 24: 129-209, 1987.
2. Lafrenie, R.M., Buchanan, M.R., and Orr, F.W. Adhesion molecules and their role in cancer metastasis. *Cell Biophysics* 23: 3-89, 1993.
3. Crissman, J.D., Hatfield, J.S., Menter, D.G., Sloane, B., and Honn, K.V. Morphological study of the interaction of intravascular tumor cells with endothelial cells and subendothelial matrix. *Cancer Res.* 48: 4065-4072, 1988.
4. Nicolson, G.L. Cancer metastasis: tumor cell and host organ properties important in metastasis to specific secondary sites. *Biochem. Biophys. Acta* 948: 175-224, 1988.
5. Li, L.M., Nicolson, G.L. and Fidler, I.J., Direct in vitro lysis of metastatic tumor cells by cytokine-activated murine vascular endothelial cells. *Cancer Res.* 51: 245-254, 1991.
6. Li, L.M., Kilbourn, R.G., Adams, J., and Fidler, I.J. Role of nitric oxide in lysis of tumor cells by cytokine-activated endothelial cells. *Cancer Res.* 51: 2531-2535, 1991.
7. Ishii, S., Mizoi, T., Kawano, K., Cay, O., Thomas, P., Nachman, A., Ford, R., Shoji, Y., Kruskal, J.B., Steele, G.Jr., and Jessup, J.M. Implantation of human colorectal carcinoma cells in the liver studied by in vivo fluorescence video microscopy. *Clin. Exp. Met.* 14: 153-164, 1996.

8. Jessup, J.M., Petrick, A.T., Toth, C.A., Ford, R., Meterissian, S., O'Hara, C.J., Steele, G Jr., and Thomas P. Carcinoembryonic antigen: enhancement of liver colonisation through retention of human colorectal carcinoma cells. *Br. J. Cancer* 67: 464-70, 1993.
9. Wagner, H.E., Thomas, P., Wolf, B.C., Zamcheck, N., Jessup, J.M. and Steele, G.D. Characterization of the tumorigenic and metastatic potential of a poorly differentiated human colon cancer cell lines. *Invasion Metastasis* 10: 253-266, 1990.
10. Jessup, J.M., Giavazzi, R., Campbell, D., Cleary, K.R., Morikawa, K., Hostetter, R., Atkinson, E.N. and Fidler, I.J. Metastatic potential of human colorectal carcinomas implanted into nude mice: prediction of clinical outcome in patients operated upon for cure. *Cancer Res.* 49: 6906-10, 1989.
11. Smedsrød, B., Pertoft, H., Eggertsen, G. and Sundstrom, C. Functional and morphological characterization of cultures of Kupffer cells and liver endothelial cells prepared by means of density separation in percoll, and selective substrate adherence. *Cell Tissue Res.* 241: 639-649, 1985.
12. Vidal-Vanaclocha, F., Rocha, M., Asumendi, A. and Barberá-Guillem, E., Isolation and enrichment of two sublobular compartment-specific endothelial cell subpopulations from liver sinusoids. *Hepatology* 18: 328-339, 1993.
13. Mørland, B., And Kaplan, G., Macrophage activation in vivo and in vitro. *Exp. Cell Res.* 108: 279-288, 1977.

14. Irving, M.G., Roll, F.J., Huang, S., and Bissell, D.M. Characterization and culture of sinusoidal endothelium from normal rat liver: lipoprotein uptake and collagen phenotype. *Gastroenterology* 87: 1233-1247, 1984.
15. Phillips, N.C., Rioux, J., And Tsao, M.S. Activation of murine Kupffer cell tumoricidal activity by liposomes containing lipophilic muramyl dipeptide. *Hepatology* 8: 1046-1050, 1988.
16. Toth, C.A., Thomas, P., Broitman, S.A. and Zamcheck, N. Receptor mediated endocytosis of carcinoembryonic antigen by rat liver Kupffer cells. *Cancer Res.* 45: 392-397, 1985.
17. Moore, P.L., MacCoubrey, I.C. and Haugland, R.P., A rapid, pH insensitive, two color fluorescence viability (cytotoxicity) assay. *J. Cell. Biol.* 111: 58a, 1990.
18. Saad, B., Frei, K., Scholl, F.A., Fontana, A. and Maier, P. Hepatocyte-derived interleukin-6 and tumor-necrosis factor α mediate the lipopolysaccharide-induced acute-phase response and nitric oxide release by cultured rat hepatocytes. *Eur. J. Biochem.* 229: 349-355, 1995.
19. Green, L.C., Wagner, D.A., Glogowski, J., Skipper, P.L., Wishnok, J.S. and Tannenbaum, S.R. Analysis of nitrate, nitrite and ^{15}N -nitrate in biological fluids. *Anal. Biochem.* 126: 131-138, 1982.
20. Oyanagi, T. Reevaluation of assay methods and establishment of kit for superoxide dismutase activity. *Anal. Biochem.* 142: 290-296, 1984.

21. Roh, M.S., Kahky, Mp., Oyedeji, C., Klostergaard, J., Wang, L., Curley, S.A. and Lotzova, E. Murine Kupffer cells and hepatic natural killer cells regulate tumor growth in a quantitative model of colorectal liver metastases. *Clin. Exp. Met.* 10: 317-27, 1992.
22. Chambers, A.F., Schmidt, E.E., Macdonald, I.C., Morris, V.L. and Groom, A.C. Early step in hematogenous metastasis of B16F1 melanoma cells in chickembryos studied by high-resolution intravital videomicroscopy. *JNCI.* 84: 797-803, 1992.
23. Rocha, M., Kruger, A., Van Rooijen, N., Schirmacher, V. and Umansky, V., Liver endothelial cells participate in T-cell-dependent host resistance to lymphoma metastasis by production of nitric oxide in vivo. *Int. J. Cancer* 63: 405-411, 1995.
24. Knook, D.L., Blansjaar, N. and Sleyster, E., Isolation and characterization of Kupffer and endothelial cells from the rat liver. *Exp. Cell Res.* 109: 317-329, 1977.
25. Steer, C.J. and Clarenburg, R. Unique distribution of glycoprotein receptors on parenchymal and sinusoidal cells of rat liver. *J. Biol. Chem.* 254: 4457-4461, 1979.
26. Alpini, G., Phillips, J.O., Vroman, B. And Larusso, N.F. Recent advances in the isolation of liver cells. *Hepatology*, 20: 494-514, 1994.
27. Smedsrød, B., Pertoft, H., Gustafson, S. and Laurent, T.C. Scavenger functions of the liver endothelial cell. *Biochim. J.* 266: 313-327, 1990.
28. Braet, F., De Zanger, R., Sasaoki, T., Baekeland, M., Janssens, P., Smedsrød, B. and Wisse, E. Assessment of a method of isolation purification, and cultivation of rat liver sinusoidal endothelial cells. *Lab. Invest.*, 70: 944-952, 1994.

29. Hirakata, Y., Kaku, M., Furuya, N., Matsumoto, T., Tateda, K., Tomono, K. and Yamaguchi, K. Effect of clearance of bacteria from the blood on the development of systemic bacteraemia in mice. *J. Medical Microbiology* 38: 337-344, 1993.
30. Obolenskaya, M., Schulze-Specking, A., Plauman, B., Frenzer, K., Freudenburg, N. and Decker, K. Nitric oxide production by cells isolation from regenerating rat liver. *Biochem. Biophys. Res. Comm.* 204: 1305-1311, 1994.
31. Forstermann, U. Biochemistry and molecular biology of nitric oxide synthase. *Arzneimittelforschung* 44: 402-407, 1994.
32. Stuehr, D.J. and Nathan, C.F., Nitric oxide: a macrophage product responsible for cytostasis and respiratory inhibition in tumor target cell. *J. Exp. Med.* 169: 1543-1555, 1989.
33. Nathan, C., Nitric oxide as a secretory product of mammalian cells. *FASEB J.* 6: 3051-3064, 1992.
34. Nathan, C. and Xie, Q.W. Nitric oxide synthases: roles, tolls, and controls. *Cell* 78: 915-919, 1994.
35. Hibbs, Jr., J.B., Taintor, R.R. and Vavrin, Z., Macrophage cytotoxicity: role for L-arginine deiminase activity and imino nitrogen to nitrite. *Science* 235: 473-476, 1987.
36. Palmer, R.M.J., Ashton, D.S. and Moncada, S. Vascular endothelial cells synthesize nitric oxide from L-arginine. *Nature* 333: 664-666, 1988.

37. Evans, C.H., Stefanovic-Racic, M. and Lancaster, J., Nitric oxide and its role in orthopaedic disease. *Clin. Ortho. Rel. Res.* 312: 275-294 (1995).
38. Blachier, F., Selamnia, M., Robert, V., M'rabet-Touil, H. And Duee, P.H. Metabolism of L-arginine through polyamine and nitric oxide synthase pathways in proliferative or differentiated human colon carcinoma cells. *Biochim. Biophys. Acta.* 1268: 255-62, 1995.
39. Chhatwal, V.J, Ngoi, S.S, Chan, S.T, Chia, Y.W. and Moochhala, S.M., Aberrant expression of nitric oxide synthase in human polyps, neoplastic colonic mucosa and surrounding peritumoral normal mucosa. *Carcinogenesis* 15: 2081-5, 1994.
40. Jenkins, D.C., Charles, I.G., Baylis, S.A., Lelchuk, R., Radomski, M.W. and Moncada, S. Human colon cancer cell lines show a diverse pattern of nitric oxide synthase gene expression and nitric oxide generation. *Brit. J. Cancer.* 70: 847-9, 1994.
41. Tepperman, B.L., Brown, J.F., Korolkiewicz, R. and Whittle, B.J., Nitric oxide synthase activity, viability and cyclic GMP levels in rat colonic epithelial cells: effect of endotoxin challenge. *J. Pharm. Exp. Ther.* 271: 1477-82, 1994.
42. Matthews, J.R., Botting, C.H., Panico, M., Morris, H.R., and Hay, R.T. Inhibition of NF-kappaB DNA binding by nitric oxide. *Nucleic Acids Res.* 24: 2236-42, 1996.
43. Packer, L. Oxidative stress, antioxidants, aging and disease. In: "Oxidative Stress and Aging", Eds. RG Cutler, L Packer, J Bertram, A. Mori. Birkhauser Verlag Publisher, Basel/Switzerland, 1995, pp. 1-14.

44. Cooney, R.V. and Morden, L.J. Cellular nitrogen oxide production: Its role in endogenous mutation and carcinogenesis. In: "Oxidative Stress and Aging", Eds. R.G. Cutler, L. Packer, J. Bertram, A. Mori. Birkhauser Verlag Publisher, Basel/Switzerland, 1995, pp. 45-52.
45. Qureshi, A., Gorey, T.F., Byrne, P., Kay, E., McKeever, J., and Hennessy, T.P. Oxygen free radical activity in experimental colonic carcinoma. *Br J Surg* 81: 1058-9, 1994.
46. Keshavarzian, A., Zapeda, D., List, T. and Mobarhan, S. High levels of reactive oxygen metabolites in colon cancer tissue: analysis by chemiluminescence probe. *Nutr Cancer* 17: 243-9, 1992.
47. Hockenberry, D.M., Oltvai, Z.N., Yin, X.-M., Milliman, C.L. and Korsmeyer, S.J. Bcl-2 functions in an antioxidant pathway to prevent apoptosis. *Cell* 75: 241-251, 1993.
48. Beno, I., Staruchova, M., Volkovova, K. and Batovsky, M. Increased antioxidant enzyme activities in the colorectal adenoma and carcinoma. *Neoplasma* 42: 265-9, 1995.
49. Mulder, T.P., Verspaget, H.W., Janssens, A.R., de Bruin, P.A., Griffioen, G. and Lamers, C.B. Neoplasia-related changes of two copper (Cu)/zinc (Zn) proteins in the human colon.. *Free Radic Biol Med* 9: 501-6, 1990.
50. Satomi, A., Murakami, S., Hashimoto, T., Ishida, K., Matsuki, M. and Sonoda, M. Significance of superoxide dismutase (SOD) in human colorectal cancer tissue: correlation with malignant intensity. *J Gastroenterol.* 30: 177-82, 1995.

51. St Clair, D.K. and Holland, J.C. Complementary DNA encoding human colon cancer manganese superoxide dismutase and the expression of its gene in human cells. *Cancer Res.* *51*: 939-43, 1991.
52. Grisham, M.B., MacDermott, R.P. and Deitch, E.A. Oxidant defense mechanisms in the human colon. *Inflammation* *14*: 669-80, 1990.
53. Squadrito, G.L. and Pryor, W.A. The formation of peroxynitrite in vivo from nitric oxide and superoxide. *Chem-Biol. Interactions* *96*: 203-206, 1995.

LEGENDS

Figure 1. Phase-contrast and fluorescence micrographs of SEC taken after cultivation 48 hr in MCDB131 medium. (x 200, Bar equals 10 μ).

A): Cultured endothelial cells display a cobble stone appearance on fibronectin coated well. Membrane ruffling is absent.

B): More than 90% positive of SEC are labeled with DiI-Ac-LDL. Observed through the rhodamine channel.

C): SEC appear to be viable as they metabolize calcein AM and are observed through the fluorescein channel..

Figure 2. Morphological changes in Clone A and CX-1 cells cocultured with SEC. Clone A (A, C, E, G) or CX-1 (B, D, F, H) were cocultured with SEC as indicated in the "Materials and Methods" for 1 hr (A and B), 24 hr (C and D), 48 hr (E and F), or alone for 24 hr (G and H). The first aggregates of 2 - 4 Clone A cells cultured with SEC were seen at 48 hr after after coculture with SEC, whereas CX-1 cells produced nearly confluent colonies by this time. The white bar is 10 μ (200x).

Figure 3. The effect of SEC on the % metabolic activity of Clone A and CX-1 cells. CRC cells were prelabelled with the fluorescent probes Rd-Dx and calcein AM as described in "Materials and Methods" and added to SEC monolayers [(●) Clone A or (○) CX-1] or cultured alone as controls [(■) Clone A or (□) CX-1]. Fluorescing tumor cells were identified at the times indicated and the % Metabolic

Activity was measured as equal to $[1 - (\text{Cells that are Calcein AM}^- / \text{Rd-Dx}^+) / \text{All Rd-Dx}^+ \text{ cells}] \times 100$. The % Metabolic Activity of Clone A/SEC cocultures decreases significantly from that of CX-1/SEC cocultures after 4 hr as detected by ANOVA and the Fisher PSLD multivariate tests of significance. P values compare co-cultures of Clone A cells with SEC to Clone A cells alone.

Figure 4. Effect of SEC coculture on the viability and recoverability of Clone A cells. Clone A / SEC cocultures were established as described in Figures 2 and 3. At 1 - 24 hr Clone A cells were recovered by trypsinization and the numbers of cells recovered determined as a percentage of the original number of Clone A cells plated (A), as a percentage of trypan blue dye-excluding viable cells (B) or as a percentage of the total viable cells that were recovered (i.e., the product of the values in A and B are expressed in (C)).

Figure 5. The effect of SEC on the Proliferation of Clone A cells. Clone A cells were placed on SEC monolayers for 1 (○), 4 (□), 8 (▲), or 24 (■) hours, recovered as described in Figure 4 and 2×10^4 viable cells cultured alone per microtiter well in fresh RPMI 1640 medium with 10% FCS for 1 - 3 days. Cell proliferation was assayed with crystal violet and compared to the proliferation of Clone A cells that had not been exposed to SEC monolayers (△). The results suggest that coculture with SEC for longer than 8 hr inhibits cell proliferation.

Figure 6. Inhibition of nitrite production and loss of toxicity to Clone A cells cocultured with SEC by treatment with a nitric oxide synthase inhibitor. NMMA (10^{-8} to 1 mM) was added to confluent SEC monolayers cocultured with Clone A cells. The % Metabolic Activity and nitrite in the spent medium were measured after 24 hr of coculture. The nitrite levels are expressed as percentage of the amount of nitrite

produced in the untreated SEC-Clone A cocultures. The reduction in nitrite production and the increase in metabolic activity of the Clone A cells was significant at ($p < 0.01$) for NMMA concentrations greater than 10^{-4} mM.

Figure 7. The Effect of NO and Superoxide Anion Donors on CRC Cell Proliferation. Clone A (●) or CX-1 (□) cells were plated at 2×10^4 cells/well in 96-well microtiter plates in complete medium and exposed to 10 - 1200 μ M of SNP (A) or SIN-1 (B) for 48 hr. Cell proliferation was then assessed by the crystal violet assay. The results suggest that SIN-1 inhibits the proliferation of Clone A, but not CX-1, cells. In contrast, SNP does not appear to have an effect on either cell line.

Table 1. Nitrite levels in human colorectal carcinoma and murine SEC co-cultures.

<u>Cell Line</u>	<u>SEC</u>	<u>Nitrite (μM)</u>
-	-	<0.1
-	+	<0.1
CX-1	-	9.4
CX-1	+	2.9
Clone A	-	<0.1
Clone A	+	8.5

- Absence of Cell line or SEC. Absence of both cell types is the medium control.

+ Presence of Cell Line or SEC as described in "Materials and Methods"

Table 2. Dexamethasone and NMMA Inhibit SEC-Mediated Toxicity

CRC Line	Substrate	Inhibitor	% Metabolic Activity	P
CX-1	None	None	99 ± 2	-
CX-1	SEC	None	97 ± 1	NS
CX-1	SEC	NMMA	ND	
CX-1	SEC	EDTA	97 ± 2	NS
CX-1	SEC	DEX	98 ± 2	NS
Clone A	None	None	99 ± 1	-
Clone A	SEC	None	72 ± 4	<0.001
Clone A	SEC	NMMA	95 ± 3	NS
Clone A	SEC	EDTA	66 ± 5	<0.001
Clone A	SEC	DEX	88 ± 5	NS

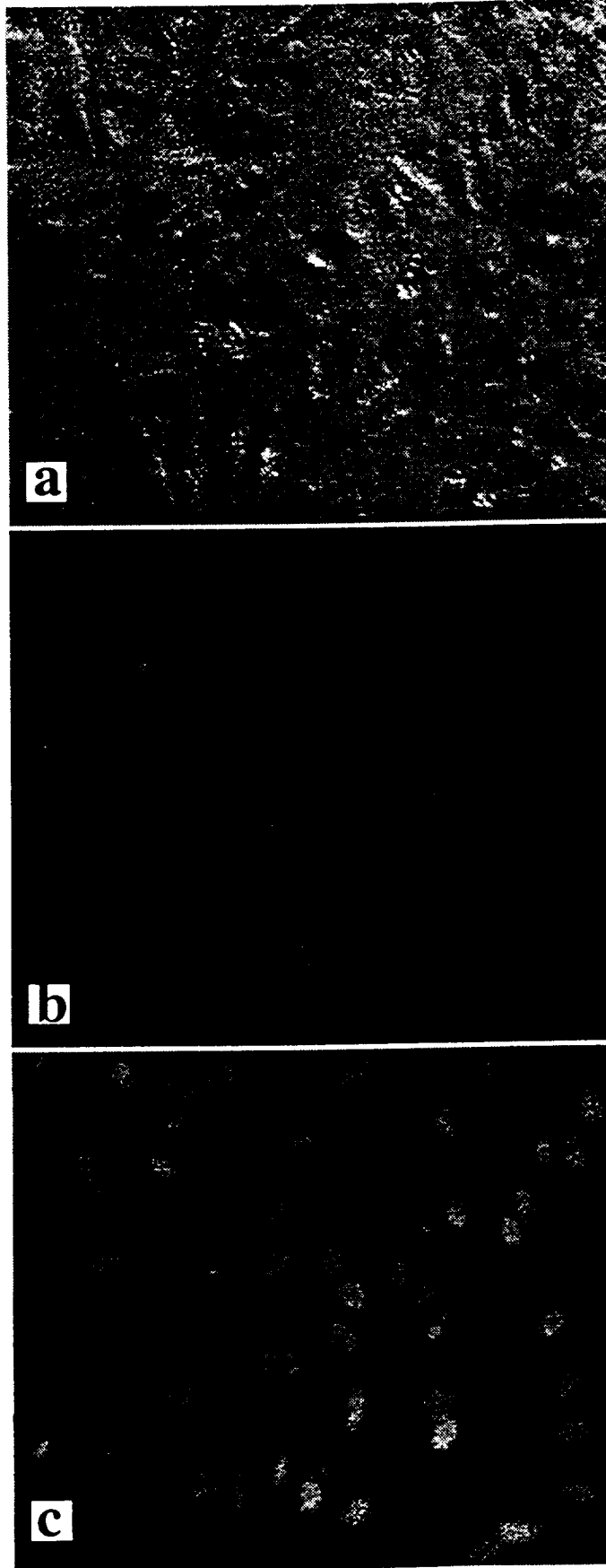
Clone A or CX-1 cells (2×10^4 cells/well) were added to microtiter wells in quadruplicate that had either confluent monolayers of SEC at ratios of 1 tumor cell: 10 SEC or no SEC (Plastic). The inhibitors were added simultaneously at 1mM NMMA, 10 mM EDTA (in medium that lacked Ca^{++}), and 10 $\mu\text{g/ml}$ dexamethasone (DEX). The % Metabolic Activity was determined after 24 hr of coculture. Mean \pm SEM are presented with comparisons to the tumor cells cultured alone. ND - not determined. NS - not significant.

Table 3. Effect of Superoxide Dismutase (SOD) and Catalase (Cat) on the Metabolic Activity of CX-1 and Clone A Carcinoma cells co-cultured With SEC

CRC Line	Substrate	Inhibitor	% Metabolic		P Value
			Activity	% Inhibition	
CX-1	None	None	86 ± 2	-	NS
CX-1	SEC	None	86 ± 2	0	-
CX-1	SEC	SOD	91 ± 2	0	NS
CX-1	SEC	Cat	94 ± 1	0	NS
Clone A	None	None	98 ± 1	-	<0.001
Clone A	SEC	None	67 ± 10	100	-
Clone A	SEC	SOD	86 ± 3	38	<0.001
Clone A	SEC	Cat	68 ± 12	95	NS

2×10^4 fluorescent dye-labeled Clone A or CX-1 cells were overlaid on SEC monolayers in the presence or absence of 1 mM SOD or catalase (Cat), incubated for 24 hr and % Metabolic Activity determined as described in "Materials and Methods".

Results are presented as Mean ± SEM with P values determined by ANOVA against the SEC-CRC positive control.



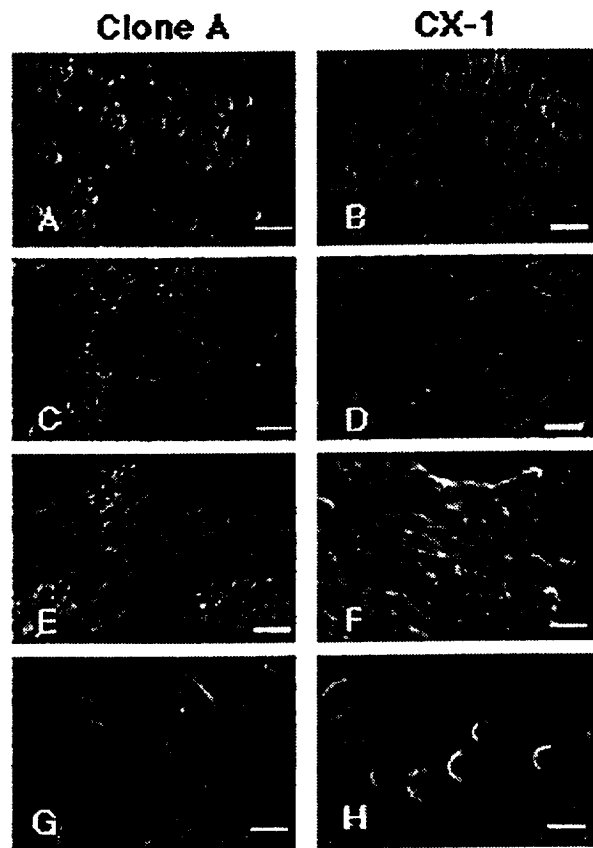


Figure 2.

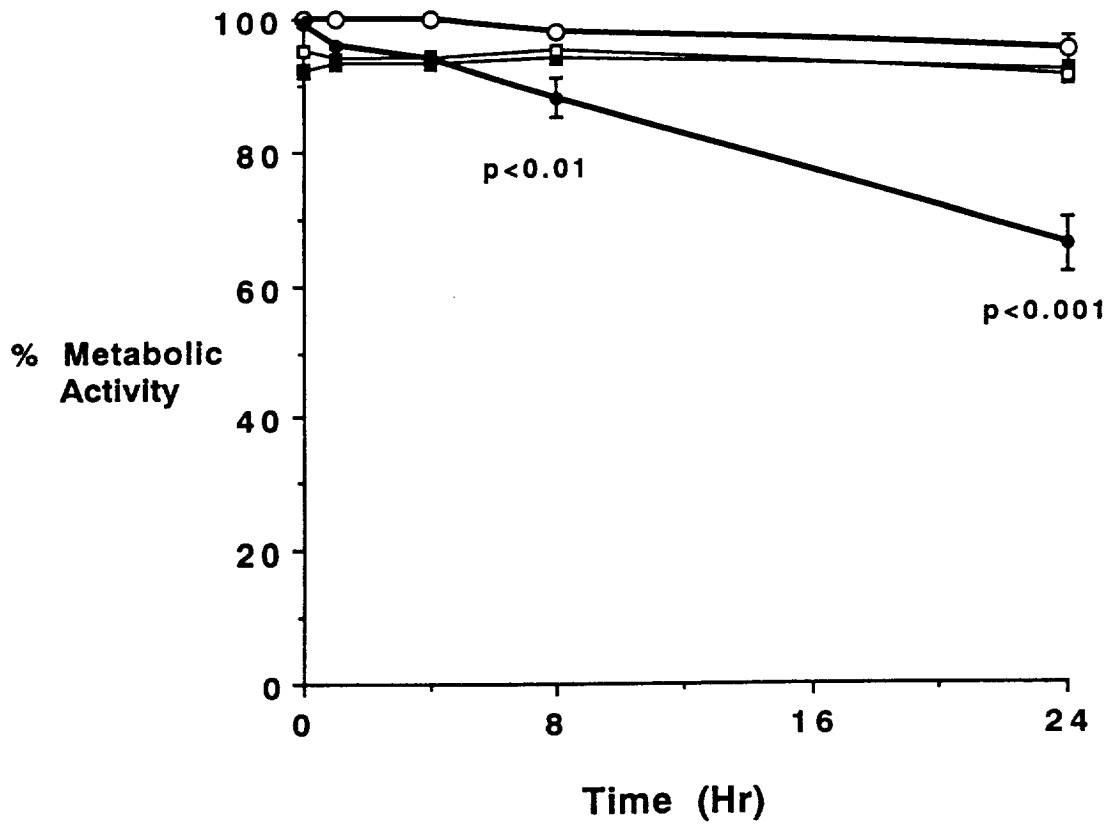


Figure 3.

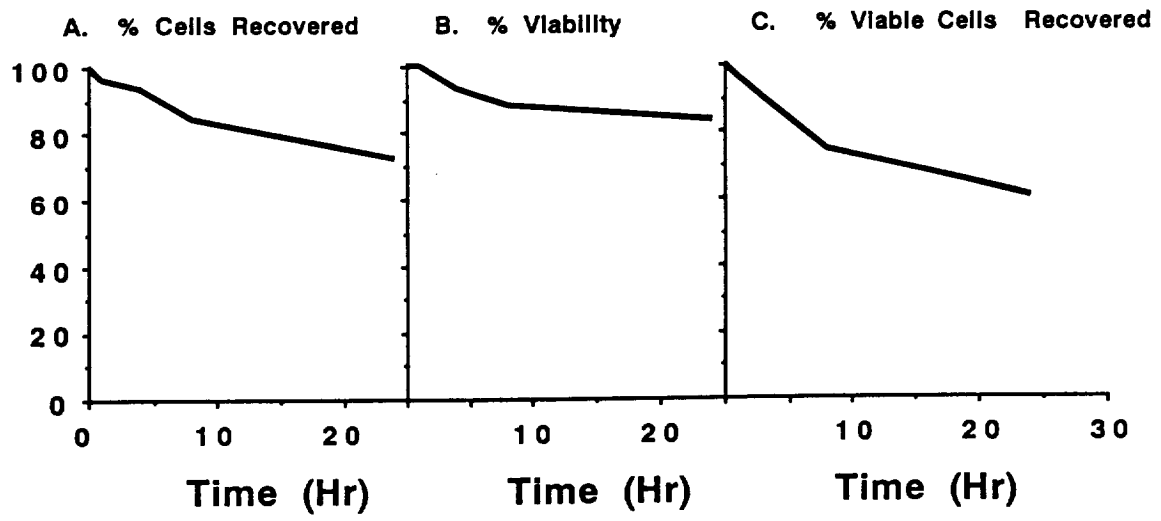


Figure 4.

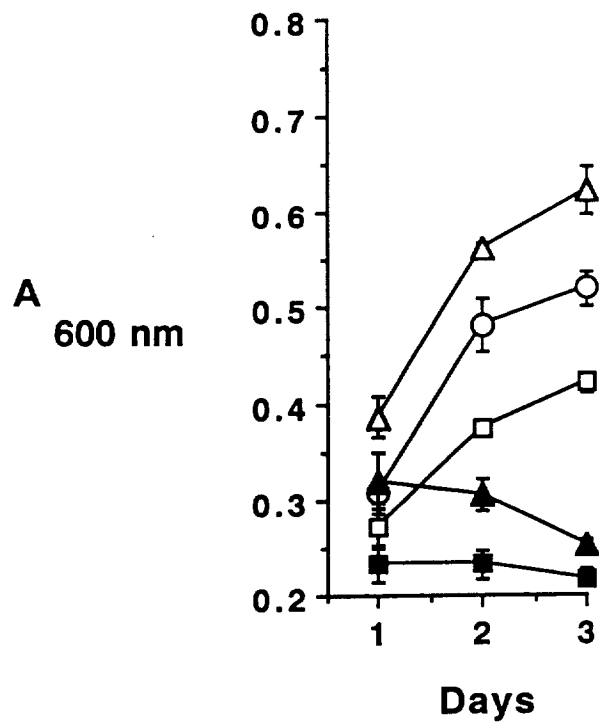


Figure 5.

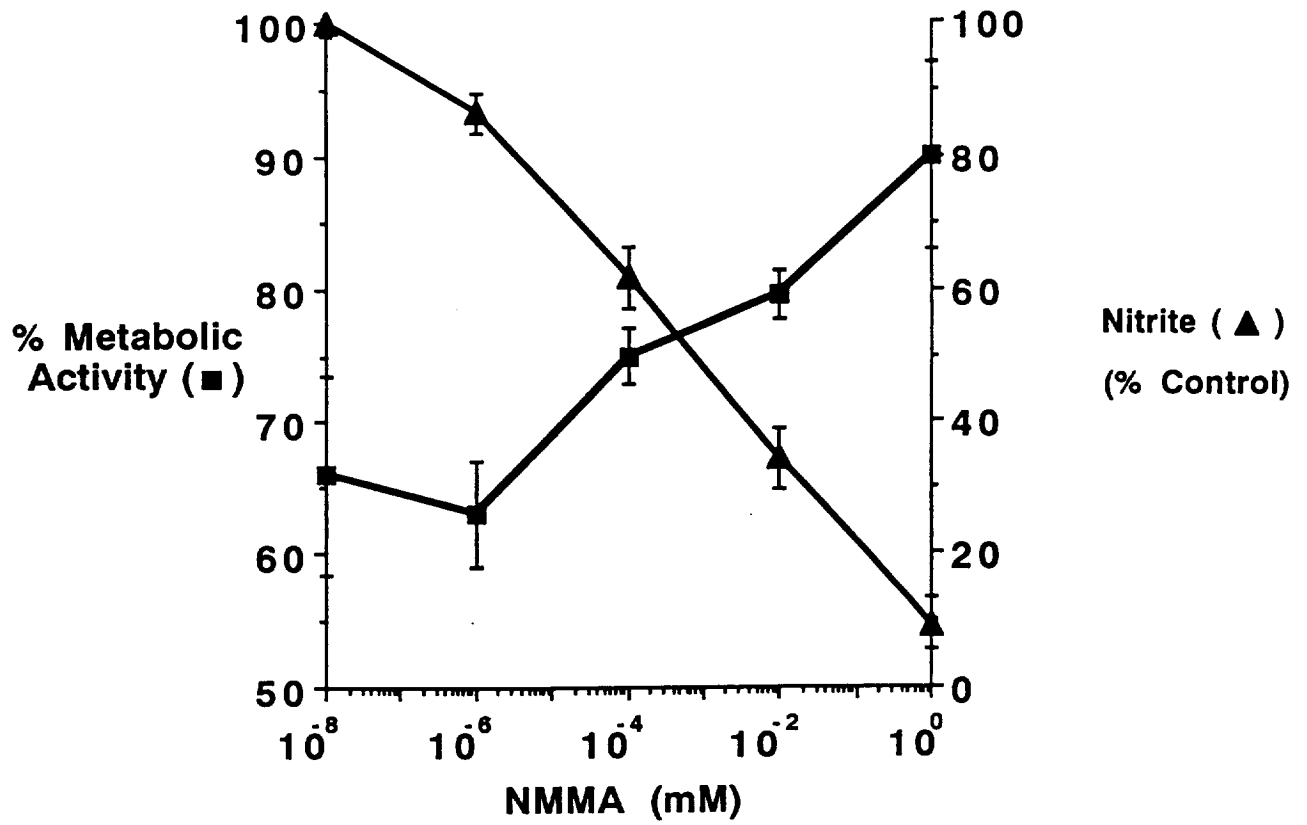


Figure 6.

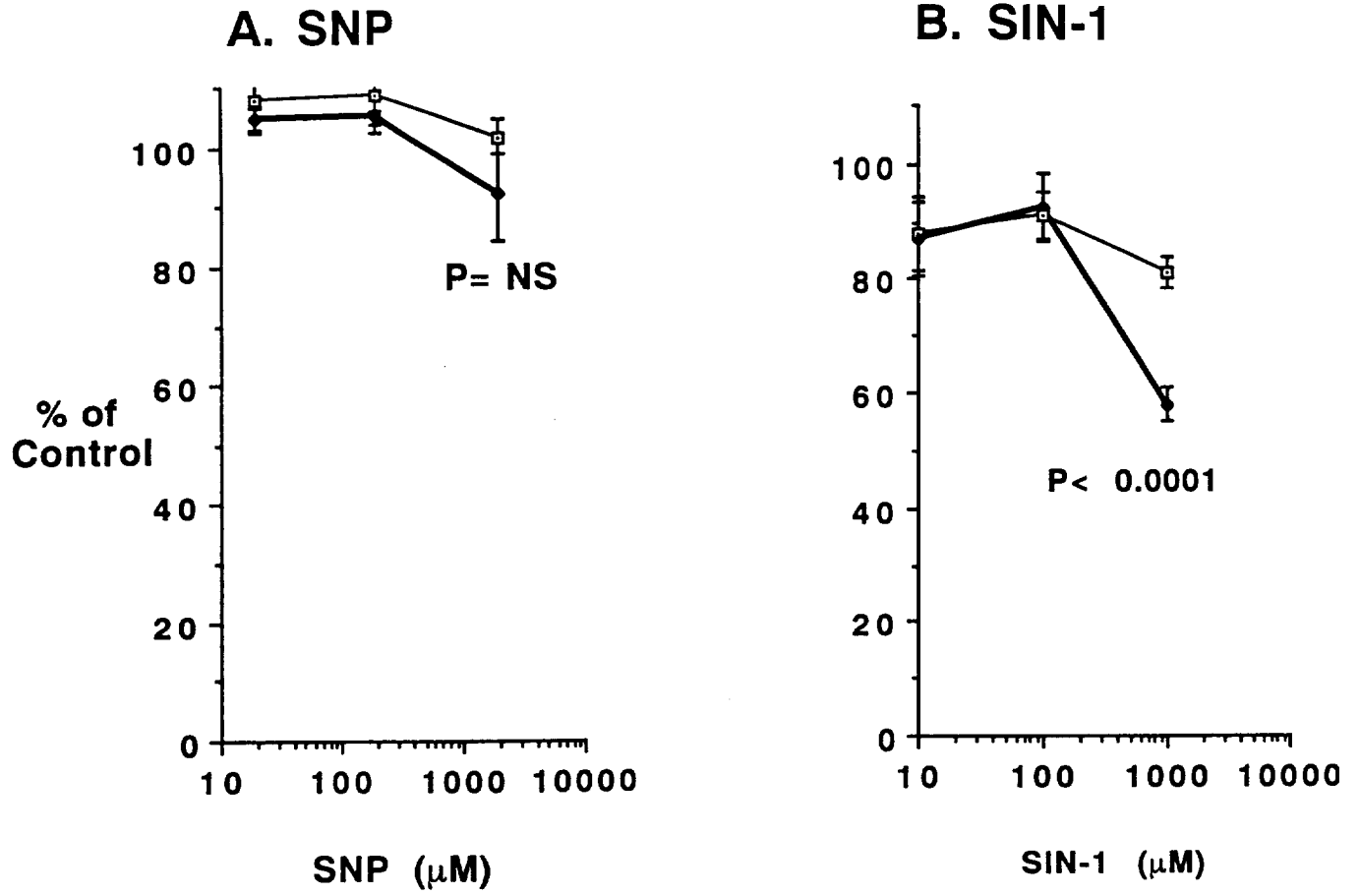


Figure 7.